Palaeogeography, Palaeoclimatology, Palaeoecology 501 (2018) 30–44

Contents lists available at ScienceDirect

Palaeogeography, Palaeoclimatology, Palaeoecology

journal homepage: www.elsevier.com/locate/palaeo

Changes in vegetation and environment in Yamzhog Yumco Lake on the southern Tibetan Plateau over past 2000 years

Chao Guo[a], Yuzhen Ma[a,*], Hongwei Meng[b], Caili Hu[a], Dandan Li[a], Jierui Liu[a], Congwen Luo[a], Kai Wang[a]

[a] State Key Laboratory of Earth Surface Processes and Resource Ecology, Faculty of Geographical Science, Beijing Normal University, Beijing 100875, China
[b] Key Laboratory of Plateau Geographical Process and Environmental Change of Yunnan Province, School of Tourism and Geographical Sciences, Yunnan Normal University, Kunming 650500, China

ARTICLE INFO

Keywords:
Late Holocene
Southern Tibetan plateau
Pollen
Medieval warm period
Little ice age
Climate change

ABSTRACT

High-resolution palynological analyses of the sediment of Yamzhog Yumco Lake can potentially provide new insight into vegetation change and climate dynamics of the southern Tibetan Plateau over the past 2000 years. The chronology, presented herein, is based on ^{210}Pb and AMS ^{14}C dates from the macro-remains of plants. Reconstruction of vegetation types, temperature and moisture indices indicate that the vegetation was alpine meadow, under relatively wet and cool conditions, from approximately 100 to 780 CE Later, the vegetation between approximately 780 and 1400 CE was alpine steppe, with a warmer and drier climate prevailing during the Medieval Warm Period (MWP). Then, the vegetation during the period from approximately 1400 to 1890 CE reverted back to alpine meadow, under relatively cold and moist climate conditions, which may have corresponded to the Little Ice Age (LIA). Since the 20th century, an alpine steppe has dominated the landscape, developed under a dry climate with a lower effective moisture. Climate records from Yamzhog Yumco Lake have confirmed a cold-moist/warm-dry climate oscillation on the southern Tibetan Plateau over the past 2000 years. Comparison of pollen records with other climatic records suggests that the climate changes in the southern Tibetan Plateau were generally similar to those in the northern Tibetan Plateau, as well as those in westerly-dominated Central Asia. Additionally, climate patterns were found to be the opposite of those in the East Asian monsoon controlled region. The temperature variations inferred from the records correlate well with changes in the solar irradiance and Northern Hemispheric temperature, which suggests a possible link between solar forcing and climate variabilities over the last 2000 years on the southern Tibetan Plateau. In addition, the enhancement and southward shift of the westerlies is determined to have significantly contributed to the high moisture conditions on the southern Tibetan Plateau during the LIA.

1. Introduction

The climatic history of the past 2000 years is of great scientific interest for understanding future climate conditions, and for assessing present and future human-induced climatic changes, which have been superimposed onto the natural trend. It is known that, over the past 2000 years, the earth's climate has experienced distinct variations on centennial timescales. This time frame includes the Medieval Warm Period (MWP, approximately 800 to 1300 CE), the Little Ice Age (LIA, approximately 1300 to 1850 CE), and the Current Warm Period (CWP, approximately 1850 CE to the present) (Mann and Jones, 2003; Mann et al., 2009; Ge et al., 2010; Ljungqvist, 2010; Christiansen and Ljungqvist, 2012). Although our knowledge regarding these centennial timescales with respect to the climatic variations has been accumulating at an accelerating rate since the 21st century, these events remain unevenly documented geographically. Therefore, the events are inadequate for depicting a reasonable global portrait.

The Tibetan Plateau is one of the earth's most imposing geomorphic features and is also one of the most sensitive areas to climate changes controlled by the interactions of large-scale atmospheric circulations, including the East Asian monsoon, Indian monsoon, and mid-latitude westerlies (Fig. 1) (Yang et al., 2003; Wang et al., 2010; An et al., 2012). Over the past several decades, many climatic records derived from ice cores, tree rings, lake sediments, and historical documents related to the last 2000 years have been recovered on the Tibetan Plateau (e.g. Thompson et al., 1995; Yang et al., 2002, 2003; Henderson et al., 2010; Zhao et al., 2010; He et al., 2013b; Lei et al., 2014). These climatic reconstructions make it possible to describe and understand

* Corresponding author at: Xueyuannan Street, #12, Haidian District, Beijing 100082, China.
E-mail address: mayzh@bnu.edu.cn (Y. Ma).

https://doi.org/10.1016/j.palaeo.2018.04.005
Received 6 November 2017; Received in revised form 10 April 2018; Accepted 10 April 2018
Available online 12 April 2018
0031-0182/

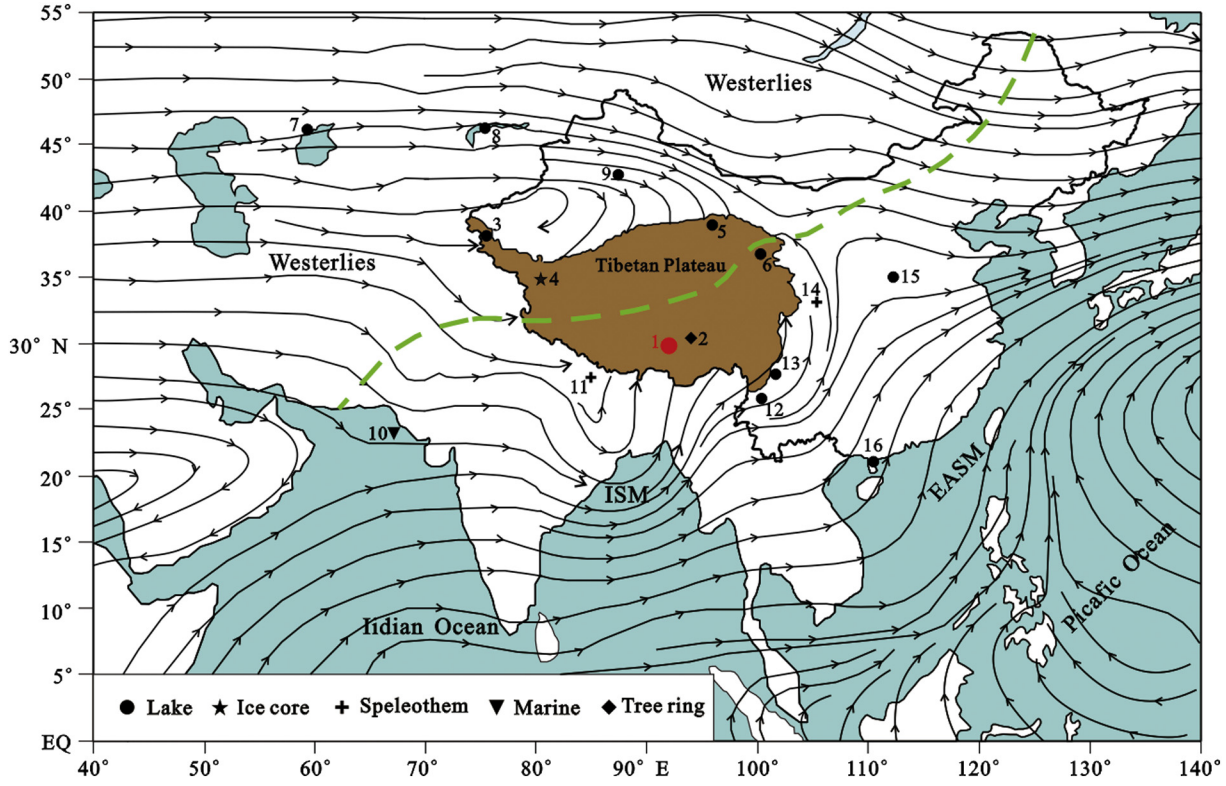

Fig. 1. Summer (June–July–August, JJA) mean 700 hPa streamline, based on the US National Centers for Environmental Prediction/National Center for Atmospheric Research (NCEP/NCAR) reanalysis during the period ranging from 1971 to 2000 CE The location of Yamzhog Yumco Lake (red solid circle) and the distribution of proxy records used in this study: 1. Yamzhog Yumco Lake (this study); 2. Linzhou Tree ring (He et al., 2013a); 3. Sasikul Lake (Lei et al., 2014); 4. Guliya Ice core (Thompson et al., 1995); 5. Sugan Lake (He et al., 2013b); 6. Qinghai Lake (Henderson et al., 2010); 7. Aral Sea (Huang et al., 2011); 8. Balkhash Lake (Feng et al., 2013); 9. Bosten Lake (Zhou, 2011); 10. NE Arabian Sea (Böll et al., 2014); 11. Sahiya Cave (Sinha et al., 2015); 12. Erhai Lake (Xu et al., 2015); 13. Lugu Lake (Sheng et al., 2015); 14. Wanxiang Cave (Zhang et al., 2008); 15. Gonghai Lake (Liu et al., 2011a); 16. Huguang Maar Lake (Yancheva et al., 2007). EASM and ISM stand for the "East Asian summer monsoon" and the "Indian summer monsoon", respectively. The green dashed line denotes the modern summer monsoon limits (from Chen et al., 2010). (For interpretation of the references to color in this figure legend, the reader is referred to the web version of this article.)

the mechanisms that have controlled or modulated the climatic changes of the Tibetan Plateau during the past 2000 years. Unfortunately, most of these investigations have been restricted to the northern and eastern sections of the Tibetan Plateau. The main focuses have been on the reconstruction of temperature, which has permitted only a limited understanding of the total climatic history of the Tibetan Plateau.

Although vegetational and climatic variations throughout the Holocene have been intensively investigated recently by several research teams (e.g., Campo and Gasse, 1993; Sun et al., 1993; Campo et al., 1996; Tang et al., 1999, 2009; Kramer et al., 2010; Herrmann et al., 2010; Kong et al., 2011; Lü et al., 2011b; Long et al., 2012; Chen et al., 2013; Leipe et al., 2014; Cheung et al., 2014), the climatic variations over the past 2000 years in the southern Tibetan Plateau have suffered from relatively lower resolution, and there remain several topics of debate. For example, on the one hand, some researchers have lent support to drier climatic conditions during the MWP and wetter conditions during the LIA (Sun et al., 1993; Morrill et al., 2003). On the other hand, other researchers have suggested an inverse pattern, with warm and wet conditions during the MWP but cold and dry conditions during the LIA (Chen et al., 2013; Cheung et al., 2014). Currently, the knowledge of the climatic changes in the southern Tibetan Plateau is far from satisfactory for depicting the temporal and spatial patterns in relation to the observed global changes over the past two millennia. Specifically, no attention has been directed toward the high-resolution or well-dated pollen sequences for the last 2000 years. Therefore, a high-resolution record of the evolution of the vegetation and climate conditions in the southern Tibetan Plateau during the last 2000 years is necessary in order to decipher and understand the complex climate changes that have occurred under the different atmospheric circulations.

The current study placed particular focus on the reconstruction of climate changes over the past 2000 years based on fossil pollen data retrieved from Yamzhog Yumco Lake, which is located in the southern section of the Tibetan Plateau. This study also compared these data with other records from the northern Tibetan Plateau, as well as those from the westerly dominated central Asian, East Asian, and the Indian summer monsoon areas. Ideally, the earlier depictions of global climate changes can be refined, and our understanding of the climate dynamics affecting the southern Tibetan Plateau during the past 2000 years can be improved upon.

2. Study site

Yamzhog Yumco Lake (28°27′ to 29°12′N, 90°08′ to 91°45′E; altitude of 4440 m above sea level) is a brackish water lake located in the southern section of the Tibetan Plateau (Fig. 1). The region is characterized by a temperate semi-arid climate. Meteorological records from a nearby weather station at Langkazi (90°24′N, 28°58′E) show that the mean annual temperature in this area is 2.6 °C, with a January mean temperature of −5.8 °C, and a July mean temperature of 9.9 °C. The mean annual precipitation is 370 mm. The records indicate that up to 85% of the annual precipitation fell during the summer seasons (June to September) for the period ranging from 1981 to 2010 CE (Fig. 2C). These data were obtained from the China Meteorological Data Sharing Service Platform (http://data.cma.cn/). In addition, the mean annual evaporation of the lake surface has reached 1290 mm (Liu, 1995). Hydrologically, Yamzhog Yumco Lake is a semi-closed lake, which is mainly recharged via precipitation and surface runoff. Six major rivers

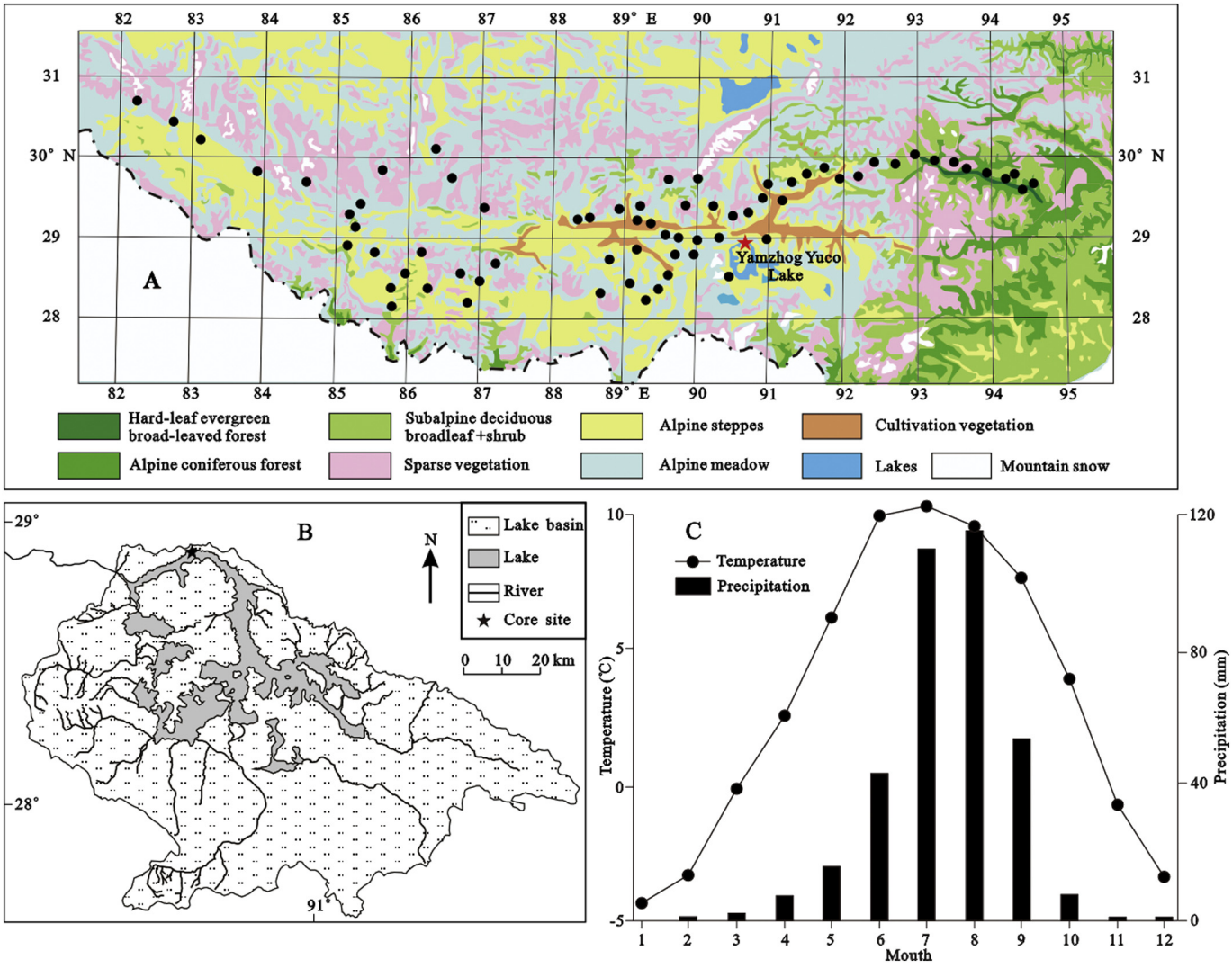

Fig. 2. Location and settings: A: Vegetation map of the southern Tibetan Plateau (the red pentagram identifies the location of Yamzhog Yumco Lake; the black filled circles indicate the sites of the modern pollen samples (from Lü et al., 2011a)); B: Map of the Yamzhog Yumco Lake Basin showing the location of the core; C: Climate diagram from the Langkazi meteorological station located near Yamzhog Yumco Lake, which includes data for the monthly averaged temperature and precipitation levels during the period ranging from 1981 to 2010 CE. (For interpretation of the references to color in this figure legend, the reader is referred to the web version of this article.)

that discharge into the lake, originating from the southern, southeastern, and western shorelines (Fig. 2B) (Sun et al., 2013b). The bedrock in the watershed mainly consists of metamorphic rock that evolved from Triassic and Cretaceous sedimentary strata (Wang et al., 1983).

The Yamzhog Yumco Lake Basin is mainly covered with alpine steppe and alpine meadow (Fig. 2A). The alpine steppes occur over an elevation belt between 4500 and 4900 m. The vegetation is mainly dominated by *Artemisia wellbyi*, *A. minor*, species of Cyperaceae (such as *Kobresia pygmaea*, *Carex montis-everestii*, *C. moorcroftii*) and species of Poaceae (*Stipa purpurea*, *S. basiplumosa*), together with *Anaphalis xylorhiza*, *Caragana versicolor*, and *Astragalus monticolus*. The alpine meadows are found between elevations of 4900 and 5200 m. The vegetation is mainly composed of *Kobresia pygmaea*, *K. humilis*, *K. royleana*, *Carex moorcroftii*, *C. oxyleuca*, accompanied by species of Poaceae (such as *Poa calliopsis*, *Stipa purpurea*, *Festuca nitidula*, *Deyeuxia tibetica*). In addition, Ranunculaceae, *Polygonum*, Caryophyllaceae, and Leguminosae are common among these vegetation types. It should be particularly noted that the coniferous and broad-leaved forests are found to grow in the valleys and mountain slopes below 4000 m in the southeastern section of the study area. Dominant species include *Pinus tabulaeformis*, *Picea crassifolia*, *Abies spectablis*, *Betula platyphylla*, *Populus davidiana*, and *Quercus liaotungensis* (Fig. 2A) (Zhang et al., 1988; Herzschuh and Birks, 2010; Lü et al., 2011a).

3. Materials and methods

3.1. Core collection

In August 2013, four 50-cm sediment cores were recovered from the northwestern basin using by a Russian drill corer (5 cm in internal diameter), as shown in Fig. 2B. The water depth at coring site was 3.2 m where far away from the estuary. The lithology in these four sediment cores correlated well with each other. The sediment cores were transported back to the laboratory in PVC pipes, where they were then described and subsampled shortly thereafter. The samples were then used for chronology, pollen, grain-size, and chemical element analyses, respectively.

3.2. Dating analysis

The chronology of the core of Yamzhog Yumco Lake was established

through ^{210}Pb analyses on the upper 19 cm of sediment and two AMS^{14}C dates from plant residues. The radioactivity of the ^{210}Pb was determined at 1-cm intervals for the upper 19 cm of the core at the Nanjing Institute of Geography and Limnology at the Chinese Academy of Sciences. Two AMS^{14}C dates from the plant residue were obtained at 32 cm and 40 cm in the core and were measured at the Beta Radiocarbon Dating Laboratory in the United States. The two AMS ^{14}C dates were calibrated to calendar years with the CALIB 6.0 program using an IntCal 13 calibration data set (Reimer et al., 2013). Then, an age-depth model of Yamzhog Yumco Lake was established based on a 2nd-order polynomial regression model. The detailed results are described in a later section.

3.3. Pollen analysis

In this study, 50 samples were obtained from the lake's core at analytical intervals of 1-cm. These samples were used for a pollen analysis at the State Key Laboratory of Earth Surface Processes and Resource Ecology, which is located at China's Beijing Normal University. One *Lycopodium* marker spore tablet (containing 9660 ± 2% exotic *Lycopodium* spores, manufactured by Lund University, batch No. 3862) was added to each sample for the purpose of calculating the total pollen concentrations prior to processing. Then, the samples were processed using HCl (10%), Na_2CO_3 (5%), HF (36%), and an acetolysis solution consisting of a 9:1 mixture of acetic anhydride and sulfuric acid to eliminate the carbonate, humid acid, silicate, and plant residues, respectively (Moore et al., 1991). Furthermore, the pollen in the residue was concentrated with a 7-μm mesh sieve, in conjunction with ultrasonic vibration. Finally, water-free glycerol was used for the storage and preparation of microscopic slides.

Pollen identification and counting were carried out using a Leica light-microscope under 400× magnification. A minimum of 300 pollen grains (average of 444 grains) were counted for each of the samples. Pollen identification was achieved with the help of key published pollen literature (Moore et al., 1991; Wang et al., 1995; Ma et al., 2009), and also by referencing an extensive modern pollen collection of more than 600 plant species from the Tibetan Plateau and western China. The Graph 10 and CorelDraw 16.0 software programs were used to plot pollen diagrams. Additionally, a cluster analysis (CONISS) was conducted to provide references for the divisions in the pollen zones.

3.4. Grain-sizes and chemical element analysis

In this study, 50 samples were collected from the lake's core at intervals of 1 cm for grain-size analysis. Approximately 0.1 g of sediment from each air-dried, disaggregated sample was pretreated with 30% H_2O_2 to remove organic matter. Then, the samples were further treated with 10% HCl, boiled to remove the carbonates, and finally washed in distilled water. The samples were then dispersed with 10% $(NaPO_3)_6$ using an ultrasonic bath for 10 min before measurements were made (Lu and An, 1997; Xiao et al., 2009). The grain-size distributions of the samples were determined with a Malvern 2000 laser diffraction instrument, with 100 bins ranging from 0.02 to 2000 μm, at the State Key Laboratory of Earth Surface Processes and Resource Ecology located at China's Beijing Normal University.

XRF core-scanning measurements were obtained directly at the split core surface of the archive half of the core using an Avaatech XRF core scanner at the School of Tourism and Geographical Sciences located at China's Yunnan Normal University. The split core surface was covered with 4-mm-thick SPEXCerti Prep Ultralene1 foil to avoid any contamination of the XRF measurement unit and desiccation of the sediment prior to the scanning XRF measurements. A Pd filter was placed in front of the incoming X-ray beam, and measurements were made at a 5-mm resolution, with a slit size of 5 × 5 cm. The generator settings were 15 kV (sample time of 10 s), 30 kV (sample time of 20 s); and 50 kV (sample time of 30 s) to obtain data for the corresponding elements: Al, Si, K, Ca, Ti, Mn, Fe, Cu, Zn, Br, Rb, Sr, Y, Zr, and Pb, respectively (Ziegler et al., 2008). The data obtained by the XRF core scanner were expressed as element intensities in counts per second (cps).

3.5. Numerical analyses

3.5.1. Non-metric multidimensional scaling

As an ordination technique, non-metric multidimensional scaling (NMS) is based on the similarity matrix between samples, as defined by a biologist, in order to reflect the particular aspects of a community structure that are biologically meaningful for a particular study (Clarke, 1993). NMS is performed to determine how the taxa distribution in all samples may be influenced by environment gradients, such as temperature and moisture gradients. NMS is often chosen for the graphical representation of community relationships, principally due to the fact that it has been found to be well suited to data that are not normal, or that lie on arbitrary, discontinuous, or otherwise questionable scales compared with other ordination techniques, such as detrended correspondence analysis (DCA), or principal components analysis (PCA). Furthermore, the use of ranked distances has been determined to improve the linearity of the relationships between the distances measured in pollen taxa and environmental spaces (Braak and Looman, 1986; Clarke, 1993; McCune and Grace, 2002). For these reasons, this technique has been used extensively in plant ecology and paleovegetation reconstruction in recent years (Soh et al., 2006; Ma et al., 2008; Simon et al., 2009; Crausbay et al., 2014). This study's non-metric multidimensional scaling procedure was conducted using Canoco 5.0 software.

3.5.2. Pollen-based quantitative climatic reconstructions

Lü et al. (2011a) established the optima and tolerance of the mean annual precipitation (MAP), July temperature (MT7), and relative humidity (HHH) of 153 pollen taxa based on 1202 modern surface pollen samples collected from the Tibetan Plateau. These three indices (MAP, MT7, and HHH) were determined based on the results of a canonical correspondence analysis (CCA), and by using locally weighted averaging (LWWA) methods (Lü et al., 2011a). Furthermore, the climatic gradient indicated by the CCA species - and sample - environment biplots was found to broadly correspond to the vegetation changes from the alpine desert, to steppe, to alpine meadow, and finally to conifer forest in the study area (Lü et al., 2011a).

In this study, based on a weighted averaging (WA) method, the optima and tolerance of the MAP, MT7, and HHH indices of 23 main pollen taxa (Table. 1) were used to reconstruct the climatic history of Yamzhog Yumco Lake Basin over the past 2000 years. It should be noted that the WA method is the basis of the ordination technique known as reciprocal averaging and is an implicit algorithm used to establish a transfer function for estimating paleo-environmental conditions from pollen assemblages (Hill, 1973; Gasse and Tekaia, 1983). Using this method, the weighted value can be weighted by each species' abundance (the percentage of each pollen species in every sample) (Hill, 1973). The WA method is often used due to the fact that it has the ability to take into account the differences in the species' abundance and ecological amplitude, which optimizes both in the pollen taxa for each sample (Braak and Looman, 1986). Additionally, in this study, SPSS. 20 software was used for the WA of the pollen spectra, and CorelDraw 16.0 software was used to produce all diagrams.

4. Results

4.1. Lithology and chronology

According to the observations and grain-size analysis, the core could be stratigraphically divided into four major units from bottom to top (Fig. 3). Sediment Unit 1 (50 to 40 cm) was a gray-brown clay-silt layer, with a silt layer at a depth of 43 to 42 cm. Sediment Unit 2 (40 to 34 cm)

Table 1
Environmental variables, optima, and tolerances of the pollen taxa of the Tibetan Plateau (Lü et al., 2011a).

Pollen taxa	MAP (mm)		HHH (%)		MT7 (°C)	
	Optima	Tolerances	Optima	Tolerances	Optima	Tolerances
Tsuga	679	240	58.5	9.6	14.8	3.6
Picea	546	188	57.7	8.4	15.2	3.4
Pinus	643	222	59.1	9.6	15.4	4
Betula	689	222	59.1	8.6	14.5	3.3
Juglans	793	218	63.9	8.9	17.1	3.6
Quercus	656	169	59.5	7.5	14.9	3.4
Salix	596	191	58.2	8.2	14.3	3.8
Ulmus	720	235	59.9	10	16.3	3.8
Oleaceae	692	300	62.3	11.5	17.5	4.4
Artemisia	384	177	51	8.8	14.2	4.2
Acer	673	250	58.3	9	15.5	3.6
Composite	444	191	53	9	13.5	4.2
Poaceae	458	217	53	9.6	14.2	4.5
Rosaceae	555	217	55.8	9.2	13.6	3.5
Polygonaceae	513	185	54.7	7.9	13.1	3.3
Polemonium	295	116	48.9	5.5	15.4	4.4
Caryophyllaceae	402	150	51.1	7.9	12.9	3.9
Liliaceae	518	219	54.5	10.1	13	4.5
Chenopodiaceae	295	161	48.5	8.7	15.2	4.7
Elaeagnus	344	178	52.2	8.4	15.9	4.8
Nitraria	271	138	48.9	7.3	16	5
Zygophyllaceae	386	40	51.7	1.9	12.7	0.5
Cyperceae	454	168	53.7	8.2	12.1	3.5

was a gray-white silt layer. Sediment Unit 3 (34 to 13 cm) was a gray-brown clay-silt layer, with three interbedded silt layers located at 32 to 29 cm, 27 to 26 cm, and 23 to 22 cm, respectively. Sediment Unit 4 (13 to 0 cm) was characterized by abundant plant roots, and it consisted of the following three subunits: Subunit 1 (13 to 7 cm) was a gray silt layer; Subunit 2 (7 to 5 cm) was a gray-white fine sand layer; and Subunit 3 (5 to 0 cm) was a gray-white medium sand layer.

The chronology of the Yamzhog Yumco Lake core was determined using ^{210}Pb analysis and AMS^{14}C dating. The dating reliability, possible problems, and age-depth model had been previously discussed

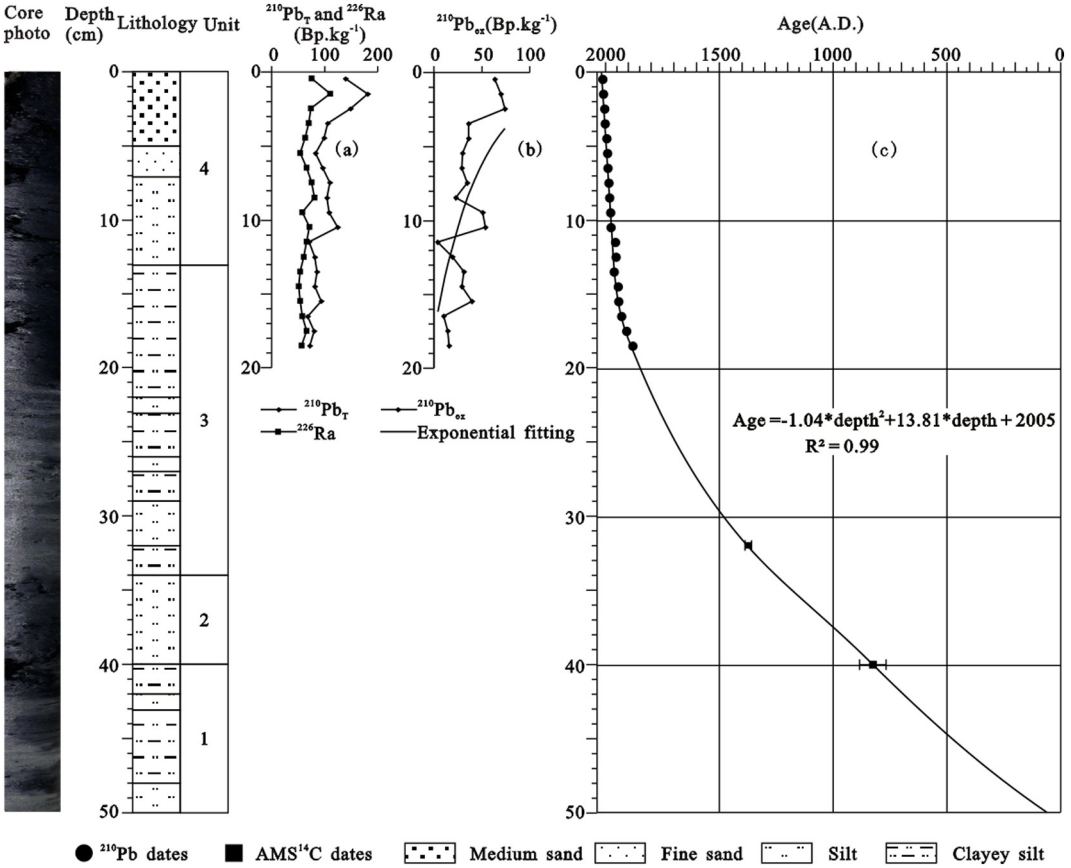

Fig. 3. Lithology, core photo, total ^{210}Pb ($^{210}Pb_T$) and ^{226}Ra radioactivity, excess ^{210}Pb ($^{210}Pb_{ex}$) radioactivity, and age-depth model of the core of Yamzhog Yumco Lake.

Table 2
AMS^{14}C ages of the Yamzhog Yumco Lake's core.

Sample number	Materials	Depth (cm)	δ^{13}C(‰)	Measured age (^{14}C yr B.P.)	Conventional age (cal yr B.P.)	2σ Calibration age. (CE)
YH-02	Plant material	32	−7.5	420 ± 30	710 ± 30	1370–1380
YH-03	Plant material	40	−5.9	900 ± 30	1210 ± 30	770–890

thoroughly by Guo et al. (2016). The chronology was established through the following procedures. ^{210}Pb was measured for surface sample dating. The total ^{210}Pb ($^{210}Pb_T$) and excess ^{210}Pb ($^{210}Pb_{ex}$) activities from the top 19 cm showed an approximately exponential decay (Fig. 3a and b), although a distinct fluctuation was observed to have existed, which may have resulted from the changes in the lithology. Based on a constant rate of supply (CRS) model (Imboden and Mariana, 1982; Benoit and Rozan, 2001), this study calculated that 19 cm was a time marker for approximately 1890 CE, as illustrated in Fig. 3c.

In this study, AMS ^{14}C was used to date the samples in the lower section. Two AMS^{14}C dates were obtained from the core plant samples taken from 32 cm and 40 cm, and the calibration ages were determined to be approximately 1375 ± 5 CE, and 830 ± 60 CE, respectively (Table 2). The δ^{13}C values (−7.5‰ and − 5.9‰) suggested that the plant residue used for the dating may have originated from aquatic plants. In most cases, the reservoir ages of aquatic plants' organic matter in lake sediment can be evaluated by the ^{14}C concentrations of living aquatic organisms (Hendy and Hall, 2006; Morrill et al., 2006). It was found that the ^{14}C content of the living aquatic plants in Yamzhog Yumco Lake (108 to 110 pMC) agreed well with that of the living terrestrial plants around the lake (106 to 110 pMC), as well as that of the tropospheric CO_2 (approximately 108 pMC) (Morrill et al., 2006; Watanabe et al., 2010). These findings suggested that the ^{14}C reservoir effect was negligible in Yamzhog Yumco Lake (Watanabe et al., 2010). The corrected radiocarbon years were then calibrated by utilizing the 2σ probability ranges in the CALIB 6.0 and IntCal 13 software (Reimer et al., 2013).

Then, the final age-depth model was generated using a 2nd-order polynomial regression model, with a 95% significance determined using the *p*-value. Next, based on the results of the model, the age of the bottom samples was extrapolated to be approximately 100 CE (Fig. 3c).

4.2. Pollen spectra

In total, 54 different types of pollen were identified from all samples analyzed in this study. These types included sixteen tree taxa and 38 herbaceous and shrub taxa (e.g., *Tsuga*, *Pinus*, *Picea*, *Betula*, *Quercus*, *Ulmus*, *Salix*, *Alnus*, *Elaeagnus*, Rosaceae, *Juglans*, *Nitraria*, Oleaceae, Poaceae, *Artemisia*, *Aster*-type, *Taraxacum*-type, *Anthemis*-type, *Echinops*-type, Chenopodiaceae, Caryophyllaceae, Zygophyllaceae, Liliaceae, Polygonaceae, *Polemonium*, Cyperaceae, etc.). The pollen record from the core of Yamzhog Yumco Lake could be divided into four pollen assemblage zones based on the CONISS results, along with the changes in the major pollen taxa (such as *Pinus*, *Artemisia*, Poaceae, Chenopodiaceae, and Cyperaceae) and pollen concentration (Fig. 4).

Pollen Zone 1 (50 to 41 cm; approximately 100 to 780 CE) was characterized by the dominance of herbaceous pollen (50 to 70%), with a relatively high percentage of summer green-tree pollen (approximately 20%). The major herbaceous pollen types included the following: Poaceae (10 to 30%), *Artemisia* (5 to 20%), Chenopodiaceae (0 to 16%), Cyperaceae (3 to 18%), and Caryophyllaceae (0 to 10%). The summer green-tree component mainly consisted of the following: *Quercus* (0 to 9%), *Juglans* (0 to 7%), *Betula* (0 to 3%), *Salix* (0 to 7%), and *Ulmus* (0 to 3%). The remainder (approximately 20%) were types of coniferous tree pollen dominated by *Pinus*.

Pollen Zone 2 (41 to 31 cm; approximately 780 to 1400 CE) was observed to be distinctive from Pollen Zone 1 due to an increased presence of *Artemisia* (15 to 40%) at the expense of that of Poaceae (10 to 20%) and Cyperaceae (3 to 10%). It should be noted that Chenopodiaceae (3 to 20%) reached its highest percentage of the entire core in this zone, which was accompanied by the lowest pollen concentration (2000 to 4000 grains/g), and a negligible amount of tree pollen (< 20%).

Pollen Zone 3 (32 to 18 cm; approximately 1350 to 1890 CE) was marked by higher percentages of Poaceae (19 to 40%) and Cyperaceae (9 to 18%) and by lower percentages of Chenopodiaceae (0 to 10%) and *Artemisia* (10 to 20%), together with some alpine meadow plants, such as Caryophyllaceae (0 to 11%) and Polygonaceae (0 to 10%). Another notable feature of Pollen Zone 3 was a striking increase in different types of coniferous pollen, including *Pinus* (3 to 32%), *Picea* (0 to 3%), and *Tsuga* (0 to 3%). Compared with that in Zones 1 and 2, the summer green-tree pollen was observed to be slightly increased (10 to 25%), accompanied by increased pollen concentrations (3000 to 7000 grains/g).

Pollen Zone 4 (18 to 0 cm; approximately 1890 CE to present) was characterized by four features. (1) decreased percentages of tree pollen (0 to 10%) and pollen concentrations (2000 to 4000 grains/g); (2) decreased percentages of Cyperaceae (0 to 10%); (3) increased percentages of *Artemisia* (10 to 40%); and (4) the appearance of xeromorphic components, such as Zygophyllaceae (0 to 10%) and *Nitraria* (0 to 5%).

4.3. Non-metric multidimensional scaling

In this study, 25 pollen taxa with an abundance of > 2% were observed in the 50 samples obtained from the core of Yamzhog Yumco Lake. The NMS procedure suggested two dimensions for the final solution. The variances explained by the first and second axes were 38% and 32.9%, respectively (Fig. 5). The pseudo-canonical correlation was found to be significant at the 0.01 level (two-tailed). The NMS ordination and the positions of the 25 pollen types on the first two axes are shown in Fig. 5.

The steppe and desert steppe plants, including *Artemisia*, Zygophyllaceae, Chenopodiaceae, *Nitraria*, *Anthemis*-type, and Liliaceae, were determined to have negative values. Additionally, the montane forest/shrubs and alpine meadow plants, such as *Picea*, *Pinus*, *Tsuga*, *Betula*, *Quercus*, *Salix*, Rosaceae, Oleaceae, *Elaeagnus*, Cyperaceae, and Polygonaceae, displayed positive values on the first axis. Therefore, the first ordination axis likely reflects the moisture gradient, in good agreement with the modern vegetation distribution of the Tibetan Plateau (Yu et al., 2001; Herzschuh and Birks, 2010).

The second axis, on which Cyperaceae, *Pinus*, and Polygonaceae displayed higher positive values, and *Artemisia*, Chenopodiaceae, *Nitraria*, and *Polemonium* had higher negative values, likely reflects the temperature gradient.

Notably, a gradient of increasing moisture with decreasing temperature could be traced diagonally from the lower left to the upper right corner (Fig. 5). The pollen types situated in the lower left of the biplots were *Artemisia* and Chenopodiaceae, which are in higher abundance in the alpine steppe of the warm and dry areas of the Tibetan Plateau (Herzschuh and Birks, 2010). In contrast to the relatively warm and dry taxa mentioned above, the pollen types placed at the top right of the biplots were relatively cold and moist taxa, such as Cyperaceae, *Pinus*, *Picea*, and Polygonaceae. These pollen types are mainly found in the alpine meadow and subalpine dark conifer forests of the

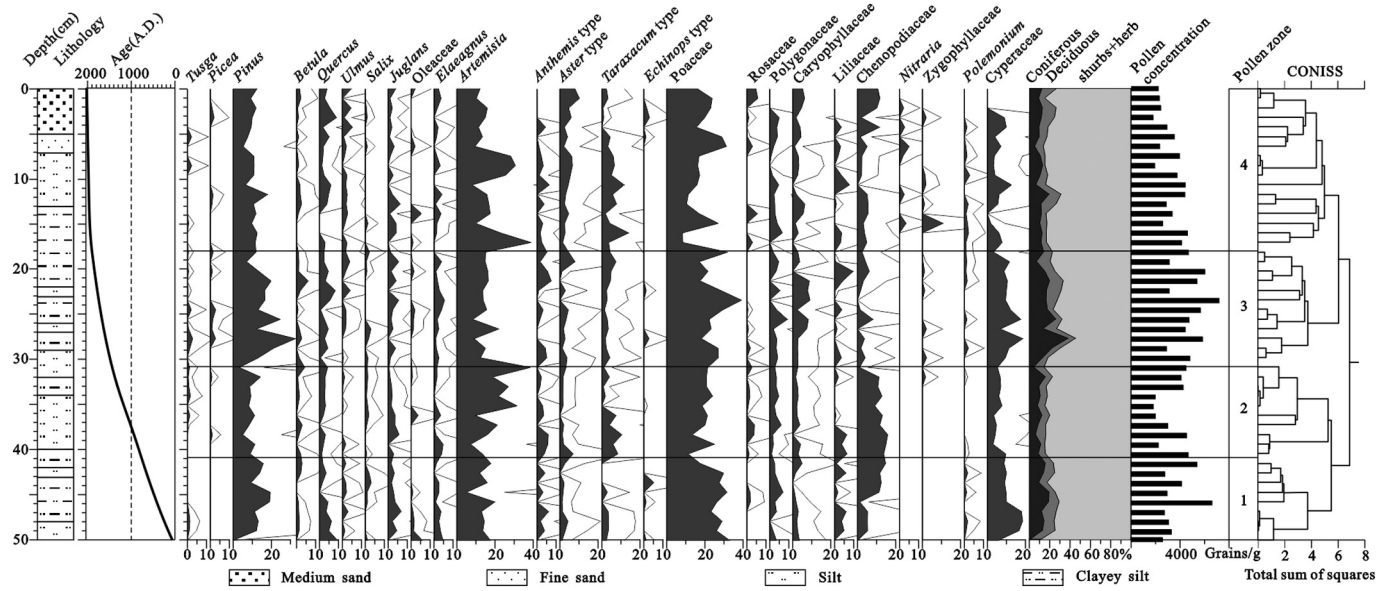

Fig. 4. Main pollen taxa percentages (black line: 5 × exaggeration); total pollen concentration; and the percentages of coniferous, deciduous, and shurbs + herbs in the core of Yamzhog Yumco Lake.

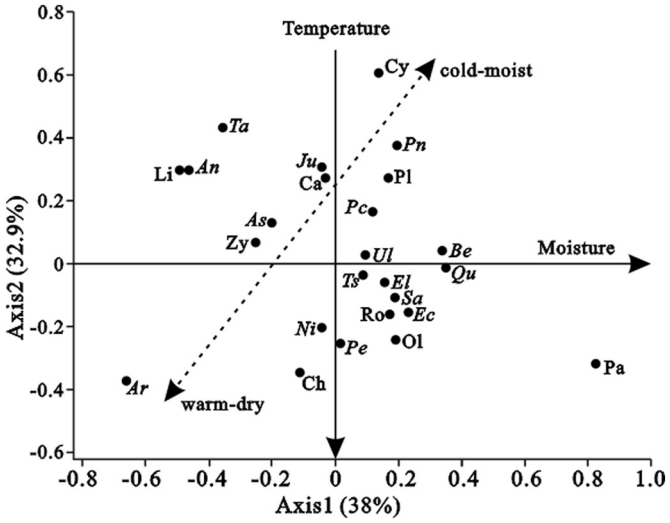

Fig. 5. Non-metric multidimensional scaling plot of the pollen taxa in a two-dimensional ordinal space. Abbreviation for pollen types: Ch, Chenopodiaceae; Zy, Zygophyllaceae; *Ni*, *Nitraria*; *Pe*, *Polemonium*; Pa, Poaceae; *Ju*, *Juglan*; *An*, *Anthemis*-type; Li, Liliaceae; *Ta*, *Taraxacum*-type; Cy, Cyperaceae; *Be*, *Betula*; *As*, *Aster*-type; Pl, Polygonaceae; *Pc*, *Picea*; *Ul*, *Ulmus*; *Pn*, *Pinus*; *Sa*, *Salix*; Ol, Oleaceae; *Ts*, *Tsuga*; *Ar*, *Artemisia*; Ro, Rosaceae; *El*, *Elaeagnus*; Ca, Caryophyllaceae; *Qu*, *Quercus*; *Ec*, *Echinops*-type.

Tibetan Plateau (Herzschuh and Birks, 2010; Lü et al., 2011a). The pollen types positioned near the center were *Betula*, *Quercus*, *Elaeagnus*, *Salix*, and Rosaceae, which have high abundance in the broad-leaf forests and mixed alpine scrub areas and thrive in the warmer and moister valleys and mountain slopes of the plateau. Therefore, the NMS results suggest that *Artemisia* could likely be used as a warm-dry pollen index and that Cyperaceae could be used as a cold-moist indicator in Yamzhog Yumco Lake Basin.

In addition, Poaceae showed a clear separation from the other plant taxa (Fig. 5), which reflected that Poaceae is able to tolerate a wide range of climatic conditions; this finding has also been indicated by the modern geographic distribution of Poaceae plants. The current results indicate that Poaceae plants have been a dominant component of alpine meadow, alpine steppe, alpine shrubland, alpine steppe-desert, and alpine desert areas on the Tibetan Plateau (Yu et al., 2001; Herzschuh and Birks, 2010).

5. Vegetation and environmental reconstructions

5.1. Proxy validation and interpretation

As previously mentioned, the pollen assemblages from the core of Yamzhog Yumco Lake were found to be dominated by Poaceae (< 40%), *Artemisia* (< 40%), *Pinus* (< 30%), Cyperaceae (< 20%), and Chenopodiaceae (< 20%) (Fig. 4). Currently, the Yamzhog Yumco Lake Basin is mainly covered with alpine steppe and alpine meadow. The alpine steppe, which is dominated by Poaceae, *Artemisia*, and Cyperaceae, occurs within an elevation belt between 4500 and 4900 m, whereas the alpine meadow, which is mainly composed of Cyperaceae and Poaceae grows in the relatively cold and moist environments between elevations of 4900 and 5200 m (Zhang et al., 1988). According to modern pollen rain studies, *Pinus* pollen is over-represented, and pine trees may not be locally present at the sites where *Pinus* pollen occurs at values < 50% (Li et al., 2005; Ma et al., 2008; Wu et al., 2013). Therefore, the *Pinus* pollen from the core of Yamzhog Yumco Lake may have been derived from the pine trees growing on the mountain slopes to the southeast of the lake.

In the modern pollen spectra derived from the non-forest vegetation (desert, steppe, and meadow) of the Tibetan Plateau, it can be observed that there is also a dominance of Chenopodiaceae, *Artemisia*, Poaceae, and Cyperaceae (Yu et al., 2001; Herzschuh and Birks, 2010). The alpine desert is characterized by high percentages of Chenopodiaceae (> 50%) and *Artemisia* (< 20%), along with a number of other taxa, including *Nitraria* and *Ephedra* (Yu et al., 2001). Samples taken from the temperate steppe have displayed significantly lower Chenopodiaceae (< 30%) values, while the percentages of *Artemisia* (> 30%) and Poaceae have been found to be higher (Yu et al., 2001). All samples from the alpine steppe showed high values of *Artemisia*, Poaceae, and Cyperaceae. Compared with those observed for the temperate steppe, the contributions of Cyperaceae, Compositae (*Anthemis*-type, *Aster*-type, and *Saussurea*-type), Caryophyllaceae, and *Thalictrum* were observed to be much higher. Additionally, it was found that Chenopodiaceae comprised less than 10% of the majority of the samples (Yu et al., 2001; Herzschuh and Birks, 2010). The samples from the alpine meadow, which covers the wet and cold mountain ranges, showed high values of

Cyperaceae, Poaceae and *Artemisia*, and also included Caryophyllaceae, Ranunculaceae, and Polygonaceae. Poaceae and *Artemisia* exhibited significantly lower values than in the samples from the alpine steppe (Yu et al., 2001; Herzschuh and Birks, 2010). Furthermore, it was observed that the Cyperaceae values increased with decreasing temperature and increasing precipitation, whereas the *Artemisia* and Poaceae values were found to be the highest at the 200- to 400-mm precipitation levels and then decreased with increasing precipitation (Shen et al., 2006; Herzschuh and Birks, 2010), in agreement with the NMS results obtained in this study. Therefore, in this study, the Cyperaceae percentage was used as an index of a cold and moist climate, and the *Artemisia* percentage was selected as an index of a warm and dry climate.

In addition, the ratios of the various pollen types have been previously used effectively as environmental indicators and can often help identify trends that may be difficult to appreciate based on percentages and concentrations alone. For example, Fowell et al. (2003) suggested the use of a semi-quantitative aridity index expressed as the ratio of desert-steppe (*Artemisia* + Chenopodiaceae) to steppe (Poaceae) taxa [(A + C) / P] for distinguishing the dry steppe from the moist meadow steppe and forest-steppe vegetation in north-central Mongolia. Accordingly, high values of the index indicated decreasing moisture availability (Fowell et al., 2003; Ma et al., 2008). Similarly, the ratio of non-arboreal pollen to arboreal pollen (NAP/AP) has been demonstrated to be an effective moisture index, particularly in sub-humid and semi-arid areas (Moore et al., 1991). Furthermore, the ratio has been used in the Russia Altai Mountain (Blyakharchuk et al., 2007), western Mongolia Plateau (Sun et al., 2013a), and Chinese Loess Plateau (Feng et al., 2006). Therefore, this study also adopted the use of (A + C) / P and (NAP/AP) as moisture indices.

The grain-size parameters of a lake's sediment can be viewed as approximate indicators of a lake's hydrological conditions, which are associated with regional climatic and environmental changes (Xiao et al., 2009). Recently, in order to provide a high-resolution proxy record of the fluctuations in lake levels, as well as environmental changes based on changes in the relative proportion of the major grain-size components, various mathematical methods have been used to define all types of grain-size distributions and partitions in the grain-size components of polymodal sediment (Xiao et al., 2009). The results obtained using these mathematical methods suggest that the fine grain-size components (approx. 7 to 10 μm) could effectively serve as sediment proxies for past changes in the levels of Yamzhog Yumco Lake, as well as moisture conditions (Guo et al., 2016).

The chemical records of a lake's sediments are the integrated result of the history of the lake's evolution, along with changes in its paleoenvironment. During the last decade, X-ray fluorescence (XRF) core scanning technologies have been developed. With these systems, it has become possible to obtain high-resolution, non-destructive, in situ XRF measurements at sub-centimeter scales (Francus et al., 2009; Kylander et al., 2011). Previous studies have demonstrated that K and Ti are typical exogenous detrital elements that increase with the enrichment of detrital inputs (Morellón et al., 2009; Metcalfe et al., 2010; Kylander et al., 2011). Furthermore, changes in Ti can be interpreted as a measure of regional rainfall, with high precipitation potentially resulting in high runoff, which favors Ti input (Yancheva et al., 2007; Shen et al., 2013). In the sediment of Yamzhog Yumco Lake, K and Ti could be used as proxies for changes in precipitation, with high values representing high precipitation, and low values representing low precipitation.

5.2. Vegetation and environmental variations over the past 2000 years

In this study, based on the pollen assemblages and semi-quantitative pollen-climate indices (Figs. 4 and 6), it was possible to reconstruct the history of vegetation changes, as well as the associated climate variations over the past 2000 years in the study area.

It was found that, from approximately 100 to 780 CE, the pollen assemblages were marked by higher percentages of Poaceae (10 to 30%) and Cyperaceae (3 to 18%), with certain amounts of *Artemisia* (5 to 20%), *Pinus* (0 to 20%), and Chenopodiaceae (0 to 16%), which likely reflected an alpine meadow vegetation under cold and moist conditions. This interpretation was based on the following two observations. First, Poaceae and Cyperaceae were documented to be under-represented in the modern pollen spectrum, whereas *Artemisia*, *Pinus*, and Chenopodiaceae were observed to be over-represented (Liu et al., 1999; Li et al., 2000; Ma et al., 2008; Wu et al., 2013). For example, the presence of Poaceae pollen, even at low percentages (3 to 10%), likely indicates the existence of grassland/steppe vegetation which is dominated by grasses, whereas the percentage of *Pinus* pollen may exceed 50% at sites where pine trees are not locally present (Liu et al., 1999; Li et al., 2005; Ma et al., 2008). Although it was found that *Artemisia* was dominant over Cyperaceae in the pollen percentages, Cyperaceae may be dominant over *Artemisia* in the vegetation abundance. This inverted relationship between *Artemisia* and Cyperaceae was found to be caused by very high pollen productivity and the well-preserved of *Artemisia* pollen (Li et al., 2005). Second, based on the distribution of the main pollen taxa on the modern pollen spectra from the Tibetan Plateau outlined above, the higher percentages of Poaceae, Cyperaceae, and *Artemisia* with the Caryophyllaceae and Polygonaceae in the palynological records, were considered to be indicative of relatively cold and moist conditions, along with widespread alpine meadow vegetation. Furthermore, the lower values of the (A + C) / P and NAP/AP ratios, relatively high values of Ti and K elements, and grain-sizes ranging from 7 to 10 μm%, lent further support to the aforementioned interpretation.

During the period ranging from approximately 780 to 1400 CE, an increased percentage of *Artemisia* (15 to 40%) at the expense of Poaceae (10 to 20%) and Cyperaceae (3 to 10%), as well as a relatively low pollen concentration, suggested that an alpine steppe landscape had probably developed under the relatively warmer and dryer conditions. Moreover, the increase in the percentages of Compositae (including *Anthemis*-type, *Aster*-type, and *Taraxacum*-type) and Chenopodiaceae (mainly at 10% levels) suggested that the interpreted alpine steppe for the period ranging between 780 and 1400 CE was similar to the modern alpine steppe in the Tibetan Plateau. In addition, the increased (A + C) / P and NAP/AP ratios, decreased grain sizes (7 to 10 μm%) and K and Ti element counts indicated that the climate during this period was dry and that the lake level had declined (Fig. 6).

It is believed that the interval between approximately 1400 and 1890 CE may have been another alpine meadow occupation interval. The pollen assemblages were characterized by increased percentages of Poaceae (19 to 40%), Cyperaceae (9 to 18%), and other meadow plants (such as Caryophyllaceae and Polygonaceae), with significant reductions in the percentages of *Artemisia* (15 to 40%) and Chenopodiaceae (< 10%). These trends most likely reflect an alpine meadow landscape. It should be noted that dramatic rises in the tree pollen percentages were observed in this period, which might suggest an expansion of the forest areas in response to the moist climate (Fig. 4). In addition, the 7 to 10 μm% peak from approximately 1400 to 1890 CE was interpreted to represent a high lake level under more humid conditions. This interpretation was corroborated by the highest Ti and K element counts, and by the lowest (A + C) / P and NAP/AP ratios, as detailed in Fig. 6.

The pollen assemblages, which were characterized by higher percentages of *Artemisia* (10 to 40%) at the expense of Cyperaceae (< 10%), along with lower pollen concentrations and the appearance of xero-herbs (such as, Zygophyllaceae and *Nitraria*), suggested that the vegetation may have been an alpine steppe under rising temperature and decreasing moisture over the most recent 100 years (Fig. 4). Furthermore, all moisture indices (including the NAP/AP ratio, (A + C) / P ratio, 7 to 10 μm%, and K and Ti counts) indicated that moisture levels have been lower during the most recent 100 years than previously (Fig. 6).

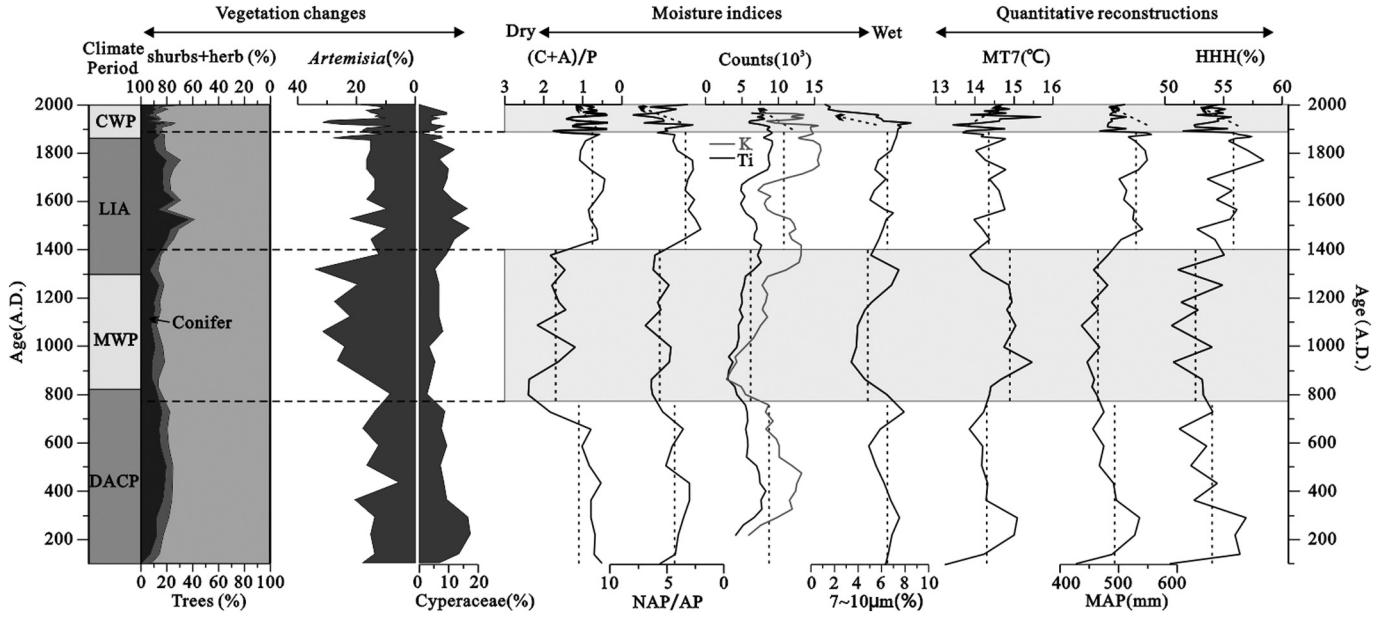

Fig. 6. Reconstruction of the vegetation and environmental condition for the core of Yamzhog Yumco Lake. The vegetation changes shown in the figure include the percentages of tree, shrubs + herb, *Artemisia*, and Cyperaceae. The moisture indices shown in the figure include the (C + A)/P ratio, NAP/AP ratio, K and Ti elements (cps), and grain-sizes of 7 to 10 μm (%). The pollen-based quantitative reconstructions indicate the July temperature (MT7), mean annual precipitation (MAP), and relative humidity (HHH). DACP, MWP, LIA, and CWP represent the Dark Age Cold Period, Medieval Warm Period, Little Lce Age, and Current Warm Period, respectively.

5.3. Pollen-based quantitative environmental reconstructions

In this study, based on the optima and tolerance of the mean annual precipitation (MAP), July temperature (MT7), and relative humidity (HHH) of the 23 major pollen taxa in the Tibetan Plateau (Lü et al., 2011a), a weighted averaging method was used to reconstruct MAP, MT7, and HHH sequences of the core of Yamzhog Yumco Lake (Fig. 6).

The results of MAP, MT7, and HHH reconstructions were found to be consistent in indicating warm and dry conditions during the Medieval Warm Period (MWP) and the Current Warm Period (CWP), and cold and moist conditions during the Dark Age Cold Period (DACP) and the Little Ice Age (LIA), as detailed in Fig. 6. Fig. 6 also shows that the climate in the study area between approximately 100 and 780 CE was relatively cold and moist, with MT7 average of approximately 14 °C, MAP average of approximately 495 mm, and HHH average of approximately 54%. During the MWP from 780 to 1400 CE, it was determined that the climate was warm and dry, with MT7 average of approximately 15 °C, MAP average of approximately 455 mm, and HHH average of approximately 52%. It was then determined that the climate shifted to cold and moist conditions toward the LIA (from approximately 1400 to 1890 CE). During this interval, the MAP fluctuated at approximately 540 mm and was clearly higher than the MWP. The HHH averaged approximately 56%, with maximum approximately 58%. Additionally, the reconstructed MT7 was found to be distinctly lower than the MWP and CWP, with an average of approximately 14 °C. It was determined that, after approximately 1890 CE, the MT7 increased, while the MAP and HHH were observed to decrease (Fig. 6).

Furthermore, it was found that the pollen-based quantitative reconstructions of the environmental history of Yamzhog Yumco Lake were also well corroborated by other environmental indices (Fig. 6). For example, the reconstructed MAP and HHH curves were observed to be nearly parallel to the moisture indices ((C + A) / P, NAP/AP, 7 to 10 μm (%), and Ti and K element counts) (Fig. 6). It should be particularly noted that the *Artemisia* pollen percentage appeared to have captured the first-order variations in MT7, and the Cyperaceae pollen percentage appeared to have captured the first-order variations in MAP and HHH. Therefore, the quantitative reconstructions and NMS results lent further support to the interpretation that the *Artemisia* pollen percentage could reasonably replicate the major variations in temperature and that the Cyperaceae pollen percentage was able to reasonably replicate the major variations in moisture (Fig. 6). Additionally, the climate pattern of Yamzhog Yumco Lake during the past 2000 years may have been a warm-dry/cold-moist pattern.

6. Discussions

As previously mentioned, this study's reconstructions indicated that the Yamzhog Yumco Lake Basin had experienced four stages of climate change over the last 2000 years. In other words, from approximately 100 to 780 CE, the basin was relatively cold and moist; from approximately 780 to 1400 CE it was warm and dry; and then it was cold and moist again between approximately 1400 and 1890 CE, with the most recent 100 years witnessing a warming and drying trend. The climate in the area was likely characterized by cold-moist and warm-dry modes. In this section, a comparison was made of the climatic changes in the Yamzhog Yumco Lake Basin during the past 1200 years with high resolution and precisely dated records from the Tibetan Plateau, as well as those from the regions of the westerly dominated central Asia, the Indian summer monsoon, and East Asian summer monsoon.

6.1. Comparison with the climate records from the Tibetan Plateau

This study's records and the interpreted results for the Yamzhog Yumco Lake Basin were found to be broadly consistent with the majority of existing records from the southern Tibetan Plateau (Sun et al., 1993; Denniston et al., 2000; Morrill et al., 2003; Tang et al., 2009; Herrmann et al., 2010; Li et al., 2011; He et al., 2013a). For instance, a tree-ring-derived millennial precipitation record from the south-central Tibetan Plateau showed higher precipitation conditions during the LIA than during the MWP (He et al., 2013a; Fig. 7A). The speleothems record in the southern margin of the Tibetan Plateau also suggested moister and cooler conditions during the LIA (Denniston et al., 2000). In addition, Morrill et al. (2003) compiled 36 previously published climate records to determine that a drier climatic condition existed

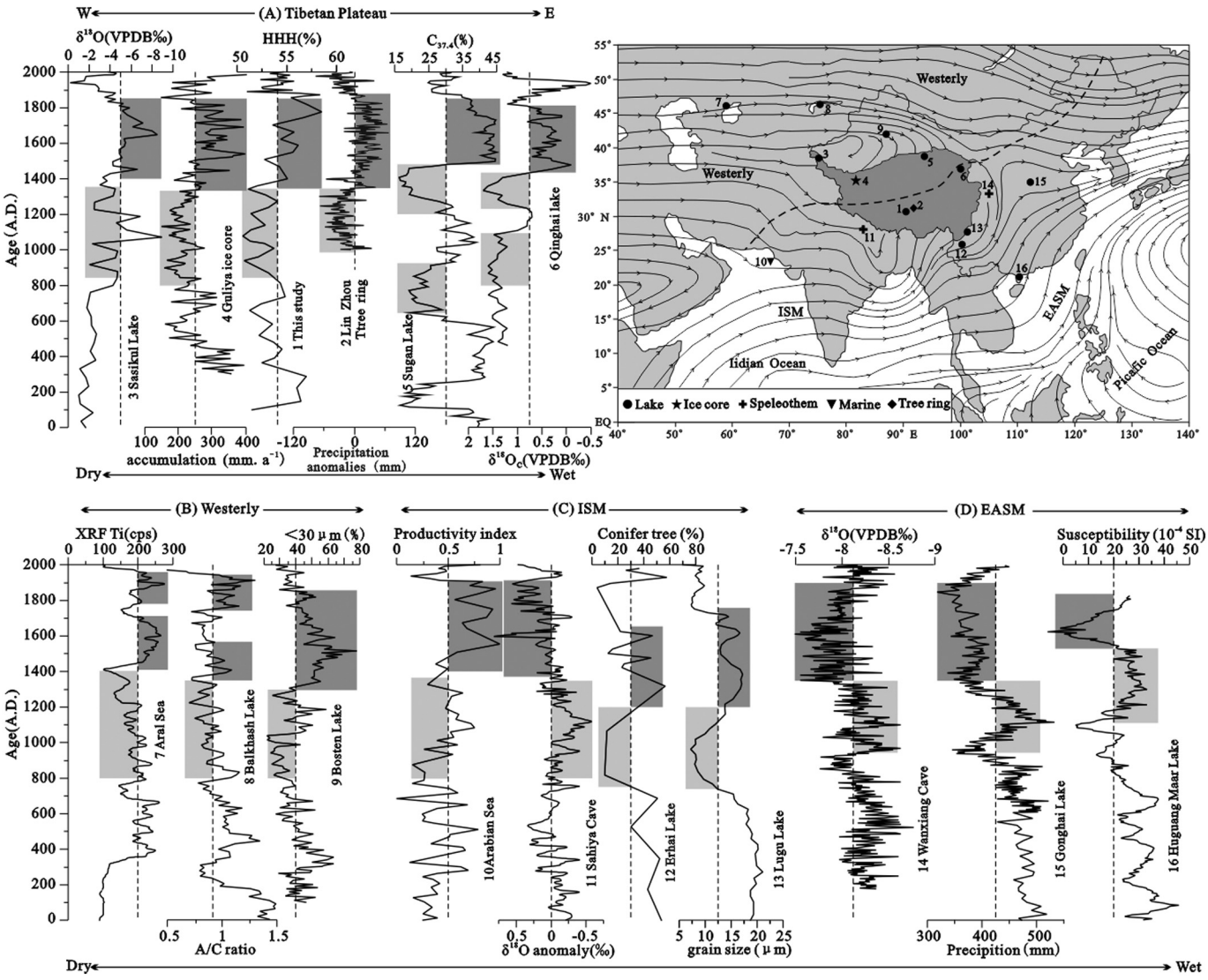

Fig. 7. Comparison of the climate history of the past 2000 years in Yamzhog Yumco Lake Basin with other records from the: (A) Tibetan Plateau; (B) Westerly-dominated regions; (C) Indian Summer Monsoon region (ISM); and (D) East Asian Summer Monsoon region (EASM). (detail see Fig. 1). The light gray squares represent the MWP, and the dark gray squares represent the LIA.

between 1000 and 1300 CE (MWP) in the southern Tibetan Plateau. The data from Namco also indicated wetter conditions during the LIA than during the MWP (Li et al., 2011). These findings may imply that a cold-moist/warm-dry association persisted over the past 2000 years in the southern Tibetan Plateau.

Furthermore, the variations in moisture at Yamzhog Yumco Lake were found to compare favorably with the lake and ice core records from the northwestern Tibetan Plateau. For example, the moisture variations in Sasikul Lake and the net mass accumulation records from the Guliya ice core indicated relatively wet conditions during the LIA (1400 to 1900 CE) and dry conditions during the MWP period (900 to 1400 CE), as well as over the most recent 100 years (Thompson et al., 1995; Lei et al., 2014; Fig. 7A). Moreover, the moisture variations at Yamzhog Yumco Lake were also determined to exhibit a trend similar to that indicated by the lacustrine records from the northeastern Tibetan Plateau. For example, the salinity variations in Sugan Lake and carbonate $\delta^{18}O$ levels in Qinghai Lake showed that a relatively high lake level existed and that increasingly effective moisture appeared between 1500 and 1840 CE However, lower lake levels and decreasingly effective moisture were determined to have occurred between 990 and 1550 CE (Henderson et al., 2010; He et al., 2013b; Fig. 7A). It should be noted that these records from northeastern Tibetan Plateau may have displayed a more pronounced fluctuation than those of the western and southern Tibetan Plateau areas during the LIA (Fig. 7A). Furthermore, the climate reflected by the lake areas and levels during the LIA was more humid than that during the MWP and CWP in other regions of the northern Tibetan Plateau (Wang et al., 2008; He et al., 2013b).

6.2. Comparison with the climate records from westerly and monsoon-controlled regions

The reconstructed climatic variations in the Yamzhog Yumco Lake Basin of the southern Tibetan Plateau were found to be similar to those indicated by the records from the westerly dominated central Asia regions. For example, the grain-size records from Bosten Lake, the A/C (*Artemisia*/Chenopodiaceae) ratio from the Balkhash Basin, and salinity reconstructions from the Aral Sea all displayed dry conditions during the MWP period (900 to 1400 CE), as well as throughout the most recent 100 to 200 years, along with relatively wet conditions from approximately 1400 to 1900 CE (Huang et al., 2011; Zhou, 2011; Feng et al., 2013; Fig. 7B). Furthermore, this cold-moist/warm-dry association may have extended to the Mediterranean Sea and Western Europe

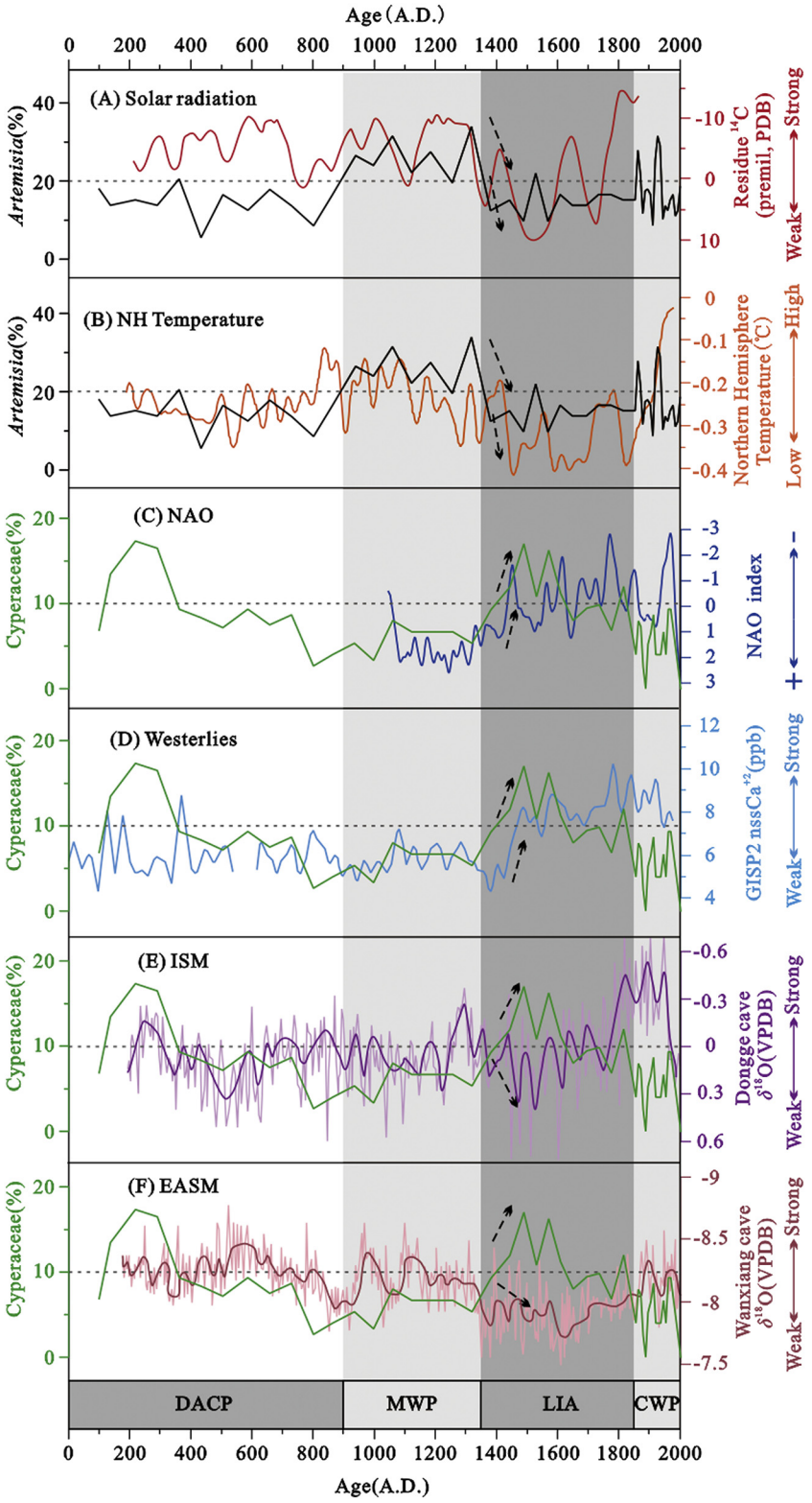

Fig. 8. Comparison of the *Artemisia* pollen percentage of Yamzhog Yumco Lake with the: (A) Solar radiation (Stuiver, 1998); and (B) Northern Hemispheric temperatures (Mann and Jones, 2003). Also, a comparison of the Cyperaceae pollen percentage of Yamzhog Yumco Lake with the: (C) North Atlantic Oscillation (NAO) index (Trouet et al., 2009); (D) Westerlies reconstruction from the GISP2 ice core (Mayewski and Maasch, 2006); (E) Indian Summer Monsoon reconstruction from Dongge Cave stalagmite $\delta^{18}O$ (thick lines indicate smoothers (span = 0.1)) (Dykoski et al., 2005); and (F) East Asian Summer Monsoon reconstruction from the Wanxiang Cave stalagmite $\delta^{18}O$ (thick lines indicate smoothers (span = 0.1)) (Zhang et al., 2008). DACP, MWP, LIA, and CWP represent the Dark Age Cold Period, Medieval Warm Period, Little Ice Age, and Current Warm Period, respectively.

(Grove, 2001; Magny et al., 2011). The similar climatic variations of the westerly dominated central Asia and Tibetan Plateau indicated that the climate changes in the Yamzhog Yumco Lake Basin may not have been a local signal, but were influenced by the larger synoptic-scale changes in atmospheric circulation.

In fact, this cold-moist/warm-dry association may not only have existed in the Tibetan Plateau and westerly controlled central Asia, but also in much wider areas controlled by the Indian Summer Monsoon (ISM) (Fig. 7C). Further evidence from a large number of proxy records in the ISM region, such as the Erhai Lake and Lugu Lake in southwestern China (Sheng et al., 2015; Xu et al., 2015; Fig. 7C), Arabian Sea (Rad et al., 1999; Böll et al., 2014; Fig. 7C), as well as equatorial eastern Africa (Verschuren, 2004; Stager et al., 2005; Hassan, 2007), support this climate pattern. That is, notably dry conditions prevailed during the MWP and CWP, and relatively humid conditions prevailed during the LIA. Nevertheless, it is noteworthy that several stalagmite $\delta^{18}O$

records from the Indian subcontinent exhibited behavior opposite that indicated by the records from the Yamzhog Yumco Lake Basin and those over most of the ISM areas on the centennial timescales. For example, the stalagmite $\delta^{18}O$ records from Sahiya Cave (Fig. 7C), Jhumar Cave, and Dandak Cave in central and northwestern India showed that wetter climate conditions prevailed during the MWP than during the LIA (Sinha et al., 2007, 2011, 2015; Berkelhammer et al., 2010; Laskar et al., 2013; Sanwal et al., 2013). However, several lines of evidence also show that the intensity of the ISM has gradually weakened and that the climate has become drier under the warmer conditions over the last 100 to 200 years (Chu et al., 2011; Sinha et al., 2011; Xu et al., 2012). These climatic contrasts in the interior ISM region were possibly related to different local and regional climatic patterns.

It should also be noted that the reconstructed climatic variations from the southern Tibetan Plateau seemed to be anti-phased relative to those from the East Asian summer monsoon (EASM) region. For example, the three absolutely dated and high-resolution climate records derived from the speleothem record (Wanxiang Cave) (Zhang et al., 2008; Fig. 7D) as well as the lake sediment (Gonghai Lake and Huguang Maar Lake) (Liu et al., 2011a; Yancheva et al., 2007; Fig. 7D) in the EASM region all implied a similar climate condition. That is, the EASM was stronger from approximately 800 to 1400 CE, as well as the last 100 to 200 years, which resulted in more humid climate conditions during the MWP and CWP. Furthermore, a weaker summer monsoon prevailed between 1400 and 1900 CE, which resulted in a drier climate condition during the LIA. Moreover, a large body of climate proxy records generally suggested an inverse relationship with this study's records from the southern Tibetan Plateau. These records originated from speleothems sediment (Hou et al., 2003; Cosford et al., 2008; Cai et al., 2010; Tan et al., 2011), lake sediment (Wang et al., 2013), swamp (Zhong et al., 2014), and historical documents (Zheng et al., 2006; Shen et al., 2009) over a wide area influenced by the EASM. Those records showed that significantly wet conditions prevailed during the MWP, as well as over the last 100 to 200 years, whereas relatively dry conditions prevailed during the LIA, which indicated a warm-wet/cold-dry pattern in the EASM region on a multi-centennial timescale.

The asynchronous variations in the climate between the westerly dominated central Asia and East Asian monsoon regions had already been identified on the millennial timescale during the Holocene (Li, 1990; Chen et al., 2008). This study's analysis confirmed that this “West-East” mode of climate variabilities may have existed not only on a millennial timescale during the Holocene, but also on a centennial timescale during the MWP and LIA. Moreover, the cold-moist/warm-dry association may have occurred not only in central Asia and northwestern China which were dominated by the westerlies (Chen et al., 2010; Chen et al., 2015), but also in the arid and semi-arid areas of the Tibetan Plateau.

6.3. Possible mechanisms

In the event that this study's reconstructions from Yamzhog Yumco Lake were able to stand further testing, a cold-moist/warm-dry climate pattern may have occurred in the southern Tibetan Plateau during the past 2000 years. Therefore, the types of mechanisms involved in producing this mode needed to be determined. In order to address these issues, this study focused on the major climate variability factors in the study region (e.g., the Solar radiation, North Hemisphere temperature, North Atlantic Oscillation (NAO) and the intensity of Westerlies, ISM and EASM) (Fig. 8). In this section, this study attempts to explore the mechanisms controlling or modulating the climate changes of the past 2000 years in the southern Tibetan Plateau, through a comparison of the pollen records from the core of Yamzhog Yumco Lake and the major climate variability factors, as presented in Fig. 8. As previously discussed, the *Artemisia* pollen percentage was able to reasonably replicate the major variations in temperature, and the Cyperaceae pollen percentage could reasonably replicate the major variations in moisture.

The warm and dry period indicated by the high percentage of *Artemisia* and low percentage of Cyperaceae spanning the MWP in Yamzhog Yumco Lake appeared to chronologically correspond with a strong period of solar radiation (Stuiver, 1998; Fig. 8A), as well as a warm period in the reconstructions of the Northern Hemispheric temperature (Mann and Jones, 2003; Fig. 8B). This study hypothesized that the relatively high solar radiation may have been the reason for the warmth and drought in the southern Tibetan Plateau during the MWP. The relatively low solar radiation during the following LIA may have lowered the temperature in the southern Tibetan Plateau, and the lowered temperature may have further increased moisture by suppressing evaporation. These opposing moisture changes, with respect to the temperature changes in the southern Tibetan Plateau, appear to be supportive of the earlier proposition that the climate in the northern Tibetan Plateau and central arid Asia region had been generally characterized by cool-wet and warm-dry modes (Liu et al., 2011b; He et al., 2013b; Lei et al., 2014; Chen et al., 2015). Within the chronological uncertainty (at least over the last 1200 years), during periods with higher solar variabilities, this study's temperature records displayed better correspondence (Fig. 8A).

The moisture history of the southern Tibetan Plateau indicated by this study's Cyperaceae pollen percentage appeared to be similar to the pattern of the westerlies (Mayewski and Maasch, 2006; Fig. 8D), suggesting that the intensity of the westerlies may have significantly contributed to the observed moisture variabilities on the southern Tibetan Plateau. Previous studies have shown that the cold temperature during the LIA would have tended to cause an enhancement and southward shift of the westerly jet stream as the meridional temperature gradient increased, which would have resulted in an increase in the occurrence of mid-latitude cyclone activities, as well as extreme precipitation events (Chen et al., 2010). In addition, the observed resemblance between the Cyperaceae percentage and the reconstructed NAO curve likely suggests that the NAO may have played an important role in shaping the pattern of the dry/moist variations in the study region at least over the past millennium (Trouet et al., 2009; Fig. 8C). That is, the wet conditions during the LIA corresponded well to a negative phase of the NAO, whereas the relatively dry conditions during the MWP corresponded to a positive phase of the NAO. As suggested by previous studies, the NAO can potentially influence the location of the jet stream and storm tracks over the North Atlantic Ocean and Eurasia (Seager et al., 2007).

When comparing this study's Cyperaceae pollen percentage with the Dongge Cave stalagmite $\delta^{18}O$ values (Fig. 8E) (Dykoski et al., 2005) and Wanxiang Cave stalagmite $\delta^{18}O$ values (Fig. 8F) (Zhang et al., 2008), it was found that the moisture history of the southern Tibetan Plateau was anti-correlated with the strength of the Asian summer monsoon at least during the last 1200 years. This study's reconstruction records imply that the lower moisture levels (or a presumably drier climate) corresponded to stronger summer monsoon and that the higher moisture levels (or a presumably wetter climate) corresponded to weaker summer monsoon (Fig. 8E and F). This association in the Yamzhog Yumco Lake Basin was observed to be exactly the opposite of the relationship identified from records in the Asian summer monsoon influenced region (Wang et al., 2010; Chen et al., 2015). The anti-phased relationship of the climatic changes potentially indicates that the Asian summer monsoon neither penetrated into the southern Tibetan Plateau nor significantly affected the moisture changes at Yamzhog Yumco Lake during at least the past millennium.

In summary, the climate changes of the southern Tibetan Plateau over the past 2000 years appeared to be a cold-moist/warm-dry association on multi-centennial timescales, with warm and dry conditions during the MWP and CWP, and cold and moist conditions during the LIA (Fig. 8). This association may be attributed to two main factors: (1) the effect of solar irradiance; and (2) the enhancement and southward shift of the westerlies during the LIA. In other words, the strong solar irradiance may have given way to higher temperature, which

strengthened the Asian summer monsoon and thereby introduced more precipitation into eastern and southern China during the MWP and CWP, resulting in a warm and wet climate. In contrast, the higher temperature could have also increased evaporation, reducing the effective moisture levels in the Tibetan Plateau, which had not been reached by the Asian summer monsoon. Therefore, the results were a warm and dry climate (He et al., 2013b; Chen et al., 2015). This anti-phased relationship could be attributed to the different responses of the balance between precipitation and evaporation to the temperature changes, which would thereby lead to opposite effective moisture changes. For the LIA, weaker solar irradiance may have given way to lower temperature, which may have effectively suppressed regional evaporation and resulted in improved effective moisture levels. At the same time, the enhancement and southward shift of the westerlies may have introduced more precipitation, resulting in a relatively moist environment.

7. Conclusions

In this study, a pollen-based reconstruction of the vegetation changes and associated climate variations at the core of Yamzhog Yumco Lake in the southern Tibetan Plateau over the past 2000 years was conducted. The reconstruction of the vegetation types, along with the temperature and moisture indices, indicated that the vegetation from approximately 100 to 780 CE was alpine meadow, dominated by Poaceae and Cyperaceae under relatively wet and cool conditions. Subsequently, the vegetation between approximately 780 and 1400 CE was alpine steppe, dominated by *Artemisia* and Poaceae, and a warm and dry climate may have occurred during the Medieval Warm Period (MWP). During the ensuing period from approximately 1400 to 1890 CE, the vegetation was replaced by alpine meadow under low temperatures and relatively high moisture conditions, which may have corresponded to the Little Ice Age (LIA). Since the 20th century, an alpine steppe has dominated the landscape in the study area. The effective moisture was quickly reduced, and a dryer climate prevailed.

The climate records from Yamzhog Yumco Lake, which is located on the southern Tibetan Plateau, confirmed the associations of warm-dry and cold-moist conditions in the region over the past 2000 years. The results are in broad agreement with records from the northern Tibetan Plateau and westerly dominated central Asia. However, the results obtained for Yamzhog Yumco Lake are found to be the opposite of those from obtained for the East Asian monsoon-controlled region.

It was determined that solar irradiance possibly played the most important role in influencing the climatic variabilities over the southern Tibetan Plateau on a multi-centennial timescale. In addition, the enhancement and southward shift of the westerlies may have contributed significantly to the high moisture conditions during the LIA.

Acknowledgments

This work was funded by the Natural Science Foundation of China (No. 41571186, 41330748), and by the National Basic Research Program of China (No. 2013CB956001).

References

An, Z., Colman, S.M., Zhou, W., Li, X., Brown, E.T., Timothy, Jull A.J., Cai, Y., Huang, Y., Lu, X., Chang, H., Song, Y., Sun, Y., Xu, H., Liu, W., Jin, Z., Liu, X., Cheng, P., Liu, Y., Ai, L., Li, X., Liu, X., Yan, L., Shi, Z., Wang, X., Wu, F., Qiang, X., Dong, J., Lu, F., Xu, X., 2012. Interplay between the Westerlies and Asian monsoon recorded in Lake Qinghai sediments since 32 ka. Sci. Rep. 2 (8), 1036.

Benoit, G., Rozan, T.F., 2001. ^{210}Pb and ^{137}Cs dating methods in lakes: a retrospective study. J. Paleolimnol. 25 (4), 455–465.

Berkelhammer, M., Sinha, A., Mudelsee, M., Cheng, H., Edwards, R.L., Cannariato, K., 2010. Persistent multi-decadal power of the Indian Summer Monsoon. Earth Planet. Sci. Lett. 290, 166–172.

Blyakharchuk, T.A., Wright, H.E., Borodavko, P.S., van der Knaap, W.O., Ammann, B., 2007. Late Glacial and Holocene vegetational history of the Altai Mountains (southwestern Tuva Republic, Siberia). Palaeogeogr. Palaeoclimatol. Palaeoecol. 245 (3), 518–534.

Böll, A., Lückge, A., Munz, P., Forke, S., Schulz, H., Ramaswamy, V., Rixen, T., Gaye, B., Emeis, K.C., 2014. Late Holocene primary productivity and sea surface temperature variations in the northeastern Arabian Sea: implications for winter monsoon variability. Paleoceanography 29 (8), 778–794.

Braak, C.J.F.T., Looman, C.W.N., 1986. Weighted averaging, logistic regression and the Gaussian response model. Plant Ecol. 65 (1), 3–11.

Cai, Y., Tan, L., Cheng, H., An, Z., Edwards, R.L., Kelly, M.J., 2010. The variation of summer monsoon precipitation in central China since the last deglaciation. Earth Planet. Sci. Lett. 291 (1–4), 21–31.

Campo, E.V., Gasse, F., 1993. Pollen- and diatom-inferred climatic and hydrological changes in Sumxi Co Basin (Western Tibet) since 13,000 yr B.P. Quat. Res. 39 (3), 300–313.

Campo, E.V., Cour, P., Hang, S., 1996. Holocene environmental changes in Bangong Co basin (Western Tibet). Part 2: the pollen record. Palaeogeogr. Palaeoclimatol. Palaeoecol. 120 (1–2), 49–63.

Chen, F.H., Yu, Z.C., Yang, M.L., Ito, E., Wang, S.M., Madsen, D.B., Huang, X.Z., Zhao, Y., Sato, T., Birks, H.J.B., Boomer, I., Chen, J.H., An, C.B., Wünnemann, B., 2008. Holocene moisture evolution in arid central Asia and its out-of-phase relationship with Asian monsoon history. Quat. Sci. Rev. 27 (3), 351–364.

Chen, F.H., Chen, J.H., Holmes, J., Boomer, I., Austin, P., Gates, J.B., Wang, N.L., Brooks, S.J., Zhang, J.W., 2010. Moisture changes over the last millennium in arid central Asia: a review, synthesis and comparison with monsoon region. Quat. Sci. Rev. 29 (7), 1055–1068.

Chen, Y., Zong, Y., Li, B., Li, S., Aitchison, J.C., 2013. Shrinking lakes in Tibet linked to the weakening Asian monsoon in the past 8.2 ka. Quat. Res. 80 (2), 189–198.

Chen, J.H., Chen, F.H., Feng, S., Huang, W., Liu, J.B., Zhou, A.F., 2015. Hydroclimatic changes in China and surroundings during the medieval climate anomaly and little ice age: spatial patterns and possible mechanisms. Quat. Sci. Rev. 107, 98–111.

Cheung, M.C., Zong, Y., Zheng, Z., Huang, K., Aitchison, J.C., 2014. A stable mid-late Holocene monsoon climate of the central Tibetan Plateau indicated by a pollen record. Quat. Int. 333 (4), 40–48.

Christiansen, B., Ljungqvist, F.C., 2012. The extra-tropical Northern Hemisphere temperature in the last two millennia: reconstructions of low-frequency variability. Clim. Past 8 (2), 765–786.

Chu, G., Sun, Q., Yang, K., Li, A., Yu, X., Xu, T., Yan, F., Wang, H., Liu, M., Wang, X., Xie, M., Lin, Y., Liu, Q., 2011. Evidence for decreasing South Asian summer monsoon in the past 160 years from varved sediment in Lake Xinluhai, Tibetan Plateau. J. Geophys. Res. 116 (D2), 347–360.

Cosford, J., Qing, H., Eglington, B., Mattey, D., Yuan, D., Zhang, M., 2008. East Asian monsoon variability since the mid-Holocene recorded in a high-resolution, absolute-dated aragonite speleothem from eastern China. Earth Planet. Sci. Lett. 275 (3), 296–307.

Crausbay, S., Genderjahn, S., Hotchkiss, S., Sachse, D., Kahmen, A., Arndt, S.K., 2014. Vegetation dynamics at the upper reaches of a tropical montane forest are driven by disturbance over the past 7300 years. Arct. Antarct. Alp. Res. 46 (46), 787–799.

Clarke, K.R., 1993. Non-parametric multivariate analyses of changes in community structure. Austral Ecol. 18 (1), 117–143.

Denniston, R.F., González, L.A., Asmerom, Y., Sharma, R.H., Reagan, M.K., 2000. Speleothem evidence for changes in Indian summer monsoon precipitation over the last ~2300 years. Quat. Res. 53 (2), 196–202.

Dykoski, C.A., Edwards, R.L., Cheng, H., Yuan, D., Cai, Y., Zhang, M., 2005. A high-resolution, absolute-dated Holocene and deglacial Asian monsoon record from Dongge cave, China. Earth Planet Sci. Lett. 233 (1–2), 71–86.

Feng, Z.D., Tang, L.Y., Wang, H.B., Ma, Y.Z., Liu, K.B., 2006. Holocene vegetation variations and the associated environmental changes in the western part of the Chinese Loess Plateau. Palaeogeogr. Palaeoclimatol. Palaeoecol. 241 (3), 440–456.

Feng, Z.D., Wu, H.N., Zhang, C.J., Ran, M., Sun, A.Z., 2013. Bioclimatic change of the past 2500 years within the Balkhash Basin, eastern Kazakhstan, Central Asia. Quat. Int. 311 (11), 63–70.

Fowell, S.J.B., Hansen, B.C.S., Peck, J.A., Khosbayar, P., Ganbold, E., 2003. Mid to late Holocene climate evolution of the Lake Telmen Basin, North Central Mongolia, based on palynological data. Quat. Res. 59 (3), 353–363.

Francus, P., Lamb, H., Nakagawa, T., Marshall, M., Brown, E., 2009. The potential of high-resolution x-ray fluorescence core scanning: applications in paleolimnology. PAGES News 17 (3), 93–95.

Gasse, E., Tekaia, E., 1983. Transfer functions for estimating paleoecological conditions (pH) from East African diatoms. Hydrobiologia 103 (1), 85–90.

Ge, Q.S., Zheng, J.Y., Hao, Z.X., Shao, X.M., Wang, W.C., Luterbacher, J., 2010. Temperature variation through 2000 years in China: an uncertainty analysis of reconstruction and regional difference. Geophys. Res. Lett. 37 (3), 93–101.

Grove, A.T., 2001. The “little ice age” and its geomorphological consequences in Mediterranean Europe. Clim. Chang. 48 (1), 121–136.

Guo, C., Ma, Y., Liu, J., Li, D., Hu, C., Pei, Q., Wu, Y., 2016. Climatic change recorded by grain-size in the past about 2000 years from Yamzhog Yumco Lake, Tibet. Quat. Sci. 36 (2), 405–419 (In Chinese with English abstract).

Hassan, F.A., 2007. Extreme Nile floods and famines in Medieval Egypt (A.D. 930–1500) and their climatic implications. Quat. Int. s 173–174 (5), 101–112.

He, M., Yang, B., Bräuning, A., Wang, J., Wang, Z., 2013a. Tree-ring-derived millennial precipitation record for the southern Tibetan Plateau and its possible driving mechanism. The Holocene 23 (1), 36–45.

He, Y., Zhao, C., Wang, Z., Wang, H., Song, M., Liu, W., Liu, Z., 2013b. Late Holocene coupled moisture and temperature changes on the northern Tibetan Plateau. Quat. Sci. Rev. 80 (80), 47–57.

Hendy, C.H., Hall, B.L., 2006. The radiocarbon reservoir effect in proglacial lakes:

examples from Antarctica. Earth Planet Sci. Lett. 241 (3–4), 413–421.
Henderson, A.C.G., Holmes, J.A., Leng, M.J., 2010. Late Holocene isotope hydrology of Lake Qinghai, NE Tibetan Plateau: effective moisture variability and atmospheric circulation changes. Quat. Sci. Rev. 29 (17–18), 2215–2223.
Herrmann, M., Lu, X., Berking, J., Schutt, B., Yao, T., Mosbrugger, V., 2010. Reconstructing Holocene vegetation and climate history of Nam Co area (Tibet), using pollen and other palynomorphs. Quat. Int. 218 (1), 45–57.
Herzschuh, U., Birks, H.J.B., 2010. Evaluating the indicator value of Tibetan pollen taxa for modern vegetation and climate. Rev. Palaeobot. Palynol. 160 (3), 197–208.
Hill, M.O., 1973. Reciprocal averaging: an eigenvector method of ordination. J. Ecol. 61 (1), 237–249.
Hou, J.Z., Tan, M., Cheng, H., Liu, T.S., 2003. Stable isotope records of plant cover change and monsoon variation in the past 2200 years: evidence from laminated stalagmites in Beijing, China. Boreas 32 (2), 304–313.
Huang, X., Oberhänsli, H., Suchodoletz, H.V., Sorrel, P., 2011. Dust deposition in the Aral Sea: implications for changes in atmospheric circulation in Central Asia during the past 2000 years. Quat. Sci. Rev. 30 (25–26), 3661–3674.
Imboden, D.M., Mariana, S., 1982. The influence of radon diffusion on the ^{210}Pb distribution in sediments. J. Geophys. Res. 87 (C1), 557–565.
Kong, P., Na, C.G., Brown, R., Fabel, D., Freeman, S., Xiao, W., Wang, W., 2011. Cosmogonic ^{10}Be and ^{25}Al dating of paleolake shorelines in Tibet. J. Asian Earth Sci. 41, 263–273.
Kramer, A., Herzschuh, U., Mischke, S., Zhang, C., 2010. Late glacial vegetation and climate oscillations on the southeastern Tibetan Plateau inferred from the Lake Naleng pollen profile. Quat. Res. 73 (2), 324–335.
Kylander, M.E., Ampel, L., Wohlfarth, B., Veres, D., 2011. High-resolution X-ray fluorescence core scanning analysis of Les Echets (France) sedimentary sequence: new insights from chemical proxies. J. Quat. Sci. 26 (1), 109–117.
Laskar, A.H., Yadava, M.G., Ramesh, R., Polyak, V.J., Asmerom, Y., 2013. A 4 kyr stalagmite oxygen isotopic record of the past Indian Summer Monsoon in the Andaman Islands. Geochem. Geophys. Geosyst. 14 (9), 3555–3566.
Lei, Y., Tian, L., Bird, B.W., Hou, J., Ding, L., Oimahmadov, I., Gadoev, M., 2014. A 2540-year record of moisture variations derived from lacustrine sediment (Sasikul Lake) on the Pamir Plateau. The Holocene 24 (7), 761–770.
Leipe, C., Demske, D., Tarasov, P.E., 2014. A Holocene pollen record from the northwestern Himalayan lake Tso Moriri: implications for palaeoclimatic and archaeological research. Quat. Int. 348, 93–112.
Li, J.J., 1990. The patterns of environmental changes since late Pleistocene in northwestern China. Quat. Sci. 3, 197–204 (In Chinese with English abstract).
Li, Y., Zhang, X., Zhou, G., 2000. Quantitative relationships between several common pollen taxa and vegetation in the north of China. Chin. Sci. Bull. 45 (7), 761–764 (In Chinese with English abstract).
Li, Y., Xu, Q., Yang, X., Zheng, Z., 2005. Pollen assemblages of major steppe communities in China. Acta Ecol. Sin. 125, 555–564 (In Chinese with English abstract).
Li, Q., Lu, H., Zhu, L., Wu, N., Wang, J., Lu, X., 2011. Pollen-inferred climate changes and vertical shifts of alpine vegetation belts on the northern slope of the nyainqentanglha mountains (central Tibetan plateau) since 8.4 kyr bp. The Holocene 21 (6), 939–950.
Liu, T., 1995. Changes of Yamzho Lake water stage in Xizang. Sci. Geogr. Sin. 15 (1), 55–62 (In Chinese).
Liu, H.Y., Cui, H., Pott, R., Speier, M., 1999. Surface pollen of the woodland-steppe ecotone in southeastern Inner Mongolia, China. Rev. Palaeobot. Palyno. 105 (3–4), 237–250.
Liu, J., Chen, F., Chen, J., Xia, D., Xu, Q., Wang, Z., Li, Y., 2011a. Humid medieval warm period recorded by magnetic characteristics of sediments from Gonghai Lake, Shanxi, North China. Chin. Sci. Bull. 56 (23), 2464–2474.
Liu, W., Liu, Z., An, Z., Wang, X., Chang, H., 2011b. Wet climate during the 'little ice age' in the arid tarim basin, northwestern China. The Holocene 3 (21), 409–416.
Ljungqvist, F.C., 2010. A new reconstruction of temperature variability in the extra-tropical Northern Hemisphere during the last two millennia. Geogr. Ann. 92 (92), 339–351.
Long, H., Lai, Z., Frenzel, P., Fuchs, M., Haberzettl, T., 2012. Holocene moist period recorded by the chronostratigraphy of a lake sedimentary sequence from Lake Tangra Yumco on the south Tibetan Plateau. Quat. Geochronol. 10 (10), 136–142.
Lu, H., An, Z., 1997. Paleoclimatic significance of grain size of loess-palaeosol deposit in Chinese loess plateau. Sci. China Ser. D Earth Sci. 41 (6), 626–631 (In Chinese).
Lü, H., Wu, N., Liu, K., Zhu, L., Yang, X., Yao, T., Wang, L., Li, Q., Liu, X., Shen, C., Li, X., Tong, G., Jiang, H., 2011a. Modern pollen distributions in Qinghai-Tibetan Plateau and the development of transfer functions for reconstructing Holocene environmental changes. Quat. Sci. Rev. 30 (7–8), 947–966.
Lü, X., Zhu, L., Nishimura, M., Morita, Y., Watanabe, T., Nakamura, T., Wang, Y., 2011b. A high-resolution environmental change record since 19 cal ka B.P. in Pumoyum Co, southern Tibet. Chin. Sci. Bull. 56 (27), 2931–2940.
Ma, Y., Liu, K., Feng, Z., Sang, Y., Wang, W., Sun, A., 2008. A survey of modern pollen and vegetation along a south–north transect in Mongolia. J. Biogeogr. 35 (8), 1512–1532.
Ma, Y., Meng, H., Sang, Y., Sun, A., Wu, J., Wang, W., 2009. Pollen keys for identification of Coniferopsida and compositae classes under light microscopy and their ecological significance. Acta. Palaeonto. Sin. 48 (2), 240–253 (In Chinese with English abstract).
Magny, M., Peyron, O., Gauthier, E., Vannière, B., Millet, L., Vermot-Desroches, B., 2011. Quantitative estimates of temperature and precipitation changes over the last millennium from pollen and lake-level data at Lake Joux, Swiss Jura Mountains. Quat. Res. 75 (1), 45–54.
Mann, M.E., Jones, P.D., 2003. Global surface temperatures over the past two millennia. Geophys. Res. Lett. 30 (15) (CLM 5-1).
Mann, M.E., Zhang, Z.H., Rutherford, S., Bradley, R.S., Hughes, M.K., Shindell, D., Ammann, C., Faluvegi, G., Ni, F.B., 2009. Global signatures and dynamical origins of the little ice age and medieval climate anomaly. Science 326 (5957), 1256–1260.
Mayewski, P.A., Maasch, K.A., 2006. Recent warming inconsistent with natural association between temperature and atmospheric circulation over the last 2000 years. Clim. Past Discuss. 2 (48), 2798–2809.
McCune, B., Grace, J.G., 2002. Analysis of Ecological Communities. MjM Software Design, Gleneden Beach, OR, pp. 125–143.
Metcalfe, S.E., Jones, M.D., Davies, S.J., Noren, A., MacKenzie, A., 2010. Climate variability over the last two millennia in the North American Monsoon region, recorded in laminated lake sediments from Laguna de Juanacatlán, Mexico. The Holocene 20 (8), 1195–1206.
Moore, P.D., Webb, J.A., Collinson, M.E., 1991. Pollen Analysis, second ed. Blackwell Scientific Publications, Oxford, pp. 163–182.
Morellón, M., Valero-Garcés, B., Vegas-Vilarrúbia, T., González-Sampériz, P., Romero, Ó., Delgado-Huertas, A., Mata, P., Moreno, A., Rico, M., Corella, J.P., 2009. Lateglacial and Holocene palaeohydrology in the western Mediterranean region: the Lake Estanya record (NE Spain). Quat. Sci. Rev. 28 (25), 2582–2599.
Morrill, C., Overpeck, J.T., Cole, J.E., 2003. A synthesis of abrupt changes in the Asian summer monsoon since the last deglaciation. The Holocene 13 (4), 465–476.
Morrill, C., Overpeck, J.T., Cole, J.E., Liu, K., Shen, C., Tang, L., 2006. Holocene variations in the Asian monsoon inferred from the geochemistry of lake sediments in Central Tibet. Quat. Res. 65 (2), 232–243.
Rad, U., Schaaf, M., Michels, K.H., Schulz, H., Berger, W.H., Sirocko, F., 1999. A 5000-yr record of climate change in varved sediments from the oxygen minimum zone off Pakistan, northeastern Arabian Sea. Quat. Res. 51 (1), 39–53.
Reimer, P.J., Bard, E., Bayliss, A., 2013. Intcal13 and marine13 radiocarbon age calibration curves 0~50,000 years cal BP. Radiocarbon 55 (4), 1869–1887.
Sanwal, J., Kotlia, B.S., Rajendran, C., Ahmad, S.M., Rajendran, K., Sandiford, M., 2013. Climatic variability in central Indian Himalaya during the last ~1800 years: evidence from a high resolution speleothem record. Quat. Int. 304 (7), 183–192.
Seager, R., Graham, N., Herweijer, C., Gordon, A.L., Kushnir, Y., Cook, E., 2007. Blueprints for medieval hydroclimate. Quat. Sci. Rev. 26 (19), 2322–2336.
Sinha, A., Cannariato, K.G., Stott, L.D., Cheng, H., Edwards, R.L., Yadava, M.G., Ramesh, R., Singh, I.B., 2007. A 900-year (600 to 1500 A.D.) record of the Indian summer monsoon precipitation from the core monsoon zone of India. Geophys. Res. Lett. 34 (16), 130–144.
Sinha, A., Stott, L., Berkelhammer, M., Cheng, H., Edwards, R.L., Buckley, B., Aldenderfer, M., Mudelsee, M., 2011. A global context for mega droughts in monsoon Asia during the past millennium. Quat. Sci. Rev. 30 (1–2), 47–62.
Sinha, A., Kathayat, G., Cheng, H., Breitenbach, S.F.M., Berkelhammer, M., Mudelsee, M., Biswas, J., Edwards, R.L., 2015. Trends and oscillations in the Indian summer monsoon rainfall over the last two millennia. Nat. Commun. 6 (8), 968–975.
Shen, C., Liu, K., Tang, L., Overpeck, J., 2006. Quantitative relationships between modern pollen rain and climate in the Tibetan Plateau. Rev. Palaeobot. Palynol. 140 (1), 61–77.
Shen, C., Wang, W.C., Peng, Y., Xu, Y., Zheng, J., 2009. Variability of summer precipitation over Eastern China during the last millennium. Clim. Past 5 (2), 129–141.
Shen, J., Wu, X., Zhang, Z., Gong, W., He, T., Xu, X., Dong, H., 2013. Ti content in Huguangyan maar lake sediment as a proxy for monsoon-induced vegetation density in the Holocene. Geophys. Res. Lett. 40 (21), 5757–5763.
Sheng, E., Yu, K., Xu, H., Lan, J., Liu, B., Che, S., 2015. Late Holocene Indian summer monsoon precipitation history at Lake Lugu, northwestern Yunnan Province, southwestern China. Palaeogeogr. Palaeoclimatol. Palaeoecol. 438, 24–33.
Simon, G., Marlowg, P., Terri, L., 2009. A new methodology for reconstructing climate and vegetation from modern pollen assemblages: an example from British Columbia. J. Biogeogr. 36 (4), 626–638.
Soh, M.C.K., Sodhi, N.S., Lim, S.L.H., 2006. High sensitivity of montane bird communities to habitat disturbance in peninsular Malaysia. Biol. Conserv. 129 (2), 149–166.
Stager, J.C., Ryves, D., Cumming, B.F., Meeker, L.D., Beer, J., 2005. Solar variability and the levels of Lake Victoria, east Africa, during the last millennium. J. Paleolimnol. 33 (2), 243–251.
Stuiver, M., 1998. INTCAL98 radiocarbon age calibration, 24,000–0\cal\, BP. Radiocarbon 40 (3), 1041–1083.
Sun, X., Du, N., Chen, Y., Gu, Z., Liu, J., Yuan, B., 1993. Holocene palynological records in lake Selincuo, Tibet. Acta Bot. Sin. 35, 943–950 (In Chinese).
Sun, A., Feng, Z., Ran, M., Zhang, C., 2013a. Pollen-recorded bioclimatic variations of the last ~22,600 years retrieved from Achit Nuur core in the western Mongolian Plateau. Quat. Int. 311, 36–43.
Sun, R., Zhang, X., Zheng, D., 2013b. Spatial variation and its causes of water chemical property in Yamzhog Yumco basin, South Tibet. Acta Geogr. Sin. 68 (1), 36–44 (In Chinese with English abstract).
Tan, L., Cai, Y., An, Z., Edwards, R.L., Cheng, H., Shen, C.C., 2011. Centennial to decadal-scale monsoon precipitation variability in the semi-humid region, northern China during the last 1860 years: records from stalagmites in huangye cave. The Holocene 21 (2), 287–296.
Tang, L., Shen, C., Liu, K., Overpeck, J.T., 1999. New high-resolution pollen records from two lakes in Xizang (Tibet). Acta Bot. Sin. 41, 896–902 (In Chinese with English abstract).
Tang, L., Shen, C., Li, C., Peng, J., Liu, H., Liu, K., Morrill, C., Overpeck, J.T., Cole, J.E., Yang, B., 2009. Pollen-inferred vegetation and environmental changes in the central Tibetan Plateau since 8200 yr BP. Sci. China Ser. D Earth Sci. 52, 1104–1114 (In Chinese with English abstract).
Thompson, L.G., Thompson, E.M., Davis, M.E., Lin, P.N., Dai, J., Bolzan, J.F., Yao, T., 1995. A 1000-year climate ice-core record from the Guliya ice cap, China: its relationship to global climate variability. Ann. Glaciol. 21, 175–181.
Trouet, V., Esper, J., Graham, N.E., Baker, A., Scourse, J.D., Frank, D.C., 2009. Persistent positive North Atlantic oscillation mode dominated the medieval climate anomaly. Science 324 (5923), 78–80.

Verschuren, D., 2004. Decadal and century-scale climate variability in tropical Africa during the past 2000 years. In: Battarbee, R.W., Gasse, F., Stickley, C.E. (Eds.), Past Climate Variability through Europe and Africa. Kluwer Academic Publishers, Dordrecht, The Netherlands, pp. 139–158.

Wang, N., Liu, G., Chen, G., 1983. Stratigraphic research of the Yamzhog Yumco region in Southern Tibet. The Qinghai-Tibet Plateau Geological Corpus 1 (6), 1–20 (In Chinese).

Wang, F., Qian, N., Zhang, Y., Yang, H., 1995. Pollen Flora of China, second ed. Science Press Publishers, Beijing, China, pp. 78–128 (In Chinese).

Wang, Y., Liu, X., Yang, X., Zhang, E., Matsumoto, R., 2008. A 4000-year moisture evolution recorded by sediments of Lake Kusai in the Hoh Xil area, northern Tibetan Plateau. J. Lake Sci. 20 (5), 605–612 (In Chinese with English abstract).

Wang, Y., Liu, X., Herzschuh, U., 2010. Asynchronous evolution of the Indian and East Asian Summer Monsoon indicated by Holocene moisture patterns in monsoonal central Asia. Earth Sci. Rev. 103 (3), 135–153.

Wang, L.C., Behling, H., Lee, T.Q., Li, H.C., Huh, C.A., Shiau, L.J., 2013. Increased precipitation during the little ice age in northern Taiwan inferred from diatoms and geochemistry in a sediment core from a subalpine lake. J. Paleolimnol. 49 (4), 619–631.

Watanabe, T., Matsunaka, T., Nakamura, T., Nishimura, M., Izutsu, Y., Minami, M., Nara, F.W., Kakegawa, T., Wang, J., Zhu, L., 2010. Last glacial–Holocene geochronology of sediment cores from a high-altitude Tibetan lake based on AMS ^{14}C dating of plant fossils: implications for paleoenvironmental reconstructions. Chem. Geol. 277 (1–2), 21–29.

Wu, J., Ma, Y., Sang, Y., Meng, H., Hu, C., 2013. Quantitative reconstruction of paleovegetation and development R-value model: an application of R-value and ERV model in Xinglong mountain natural protection region. Quat. Sci. 33 (3), 554–564 (In Chinese with English abstract).

Xiao, J., Chang, Z., Si, B., Qin, X., Itoh, S., Lomtatidze, Z., 2009. Partitioning of the grain-size components of Dali Lake core sediments: evidence for lake-level changes during the Holocene. J. Paleolimnol. 42 (2), 249–260.

Xu, H., Hong, Y., Hong, B., 2012. Decreasing Asian summer monsoon intensity after 1860 A.D. in the global warming epoch. Clim. Dyn. 39 (7–8), 2079–2088.

Xu, H., Zhou, X., Lan, J., Liu, B., Sheng, E., Yu, K., Cheng, P., Wu, F., Hong, B., Yeager, K.M., Xu, S., 2015. Late Holocene Indian summer monsoon variations recorded at Lake Erhai, Southwestern China. Quat. Res. 83 (2), 307–314.

Yancheva, G., Nowaczyk, N.R., Mingram, J., Dulski, P., Schettler, G., Negendank, J.W., Liu, J., Sigman, D.M., Peterson, L.C., Haug, G.H., 2007. Influence of the intertropical convergence zone on the East Asian monsoon. Nature 445 (7123), 74–77.

Yang, B., Brauning, A., Johnson, K.R., Shi, Y.F., 2002. General characteristics of temperature variation in China during the last two millennia. Geophys. Res. Lett. 29 (9), 381–384.

Yang, B., Brauning, A., Shi, Y.F., 2003. Late Holocene temperature fluctuations on the Tibetan Plateau. Quat. Sci. Rev. 22 (21 − 22), 2335–2344.

Yu, G., Tang, L.Y., Yang, X.D., Ke, X.K., Hassisong, S.P., 2001. Modern pollen samples from alpine vegetation on the Tibetan Plateau. Glob. Ecol. Biogeogr. 10 (5), 503–519.

Zhang, J., Wang, J.T., Chen, W., Li, B., Zhao, K., 1988. Vegetation of Xizang (Tibet), 1st ed. Science Press Publishers, Beijing, China, pp. 182–208 (In Chinese).

Zhang, P., Cheng, H., Edwards, R.L., Chen, F., Wang, Y., Yang, X., Liu, J., Tan, M., Wang, X., Liu, J., An, C., Dai, Z., Zhou, J., Zhang, D., Jia, J., Jin, L., Johnson, K.R., 2008. A test of climate, sun, and culture relationships from an 1810-year Chinese cave record. Science 322 (5903), 940–942.

Zhao, Y., Yu, Z., Liu, X., Zhao, C., Chen, F., Zhang, K., 2010. Late Holocene vegetation and climate oscillations in the Qaidam Basin of the northeastern Tibetan Plateau. Quat. Res. 73 (1), 59–69.

Zheng, J., Wang, W., Ge, Q., Man, Z., Zhang, P., 2006. Precipitation variability and extreme events in eastern China during the past 1500 years. Terr. Atmos. Ocean. Sci. 17 (3), 579–592.

Zhong, W., Xue, J., Ouyang, J., Cao, J., Peng, Z., 2014. Evidence of late Holocene climate variability in the western nanling mountains, south China. J. Paleolimnol. 52 (1–2), 1–10.

Zhou, G., 2011. Bosten Lake Recorded Climate Change of Arid Area of Northwestern China Over Last 2 ka. China (PhD Thesis) LZU, Lanzhou. (In Chinese).

Ziegler, M., Jilbert, T., De Lange, G.J., Lourens, L.J., Reichart, G., 2008. Bromine counts from XRF scanning as an estimate of the marine organic carbon content of sediment cores. Geochem. Geophys. Geosyst. 9 (5), 303–307.